IN THE UNITED STATES PATENT AND TRADEMARK OFFICE
PATENT EXAMINING OPERATION

Applicant(s): Glen H. ERIKSON et al.

Serial No: 09/713,177 Group Art Unit: 1637

Filed: November 15, 2000 Examiner: S. Chunduru

Att. Docket No.: E1047/20048 Confirmation No.: 3217

For: TRIPLEX AND QUADRUPLEX CATALYTIC HYBRIDIZATION

DECLARATION UNDER 37 C.F.R. § 1.132

Commissioner for Patents
Washington, DC 20231

Sir:

I, J. Hans van de Sande, Ph.D., a citizen of Canada, hereby declare and state:

1. The curriculum vitae attached as Exhibit A accurately reflects my professional credentials. As noted in Exhibit A, I am presently Vice-Dean of the Faculty of Medicine as well as a Professor in the Department of Biochemistry & Molecular Biology (formerly known as the Department of Medical Biochemistry) at the University of Calgary in Calgary, Alberta, Canada.

2. I am a paid consultant of Ingeneus Corp. through my association with Genetic Diagnostics, Inc., a licensee of technology owned by Ingeneus Corp. I expect to be compensated for my time expended preparing this document.

3. Prior to executing this Declaration, I reviewed the above-identified application, the June 5, 2002 Final Rejection, the January 18, 2002 DECLARATION UNDER 37 C.F.R. § 1.132 of Jasmine I. Daksis, and the January 21, 2002 DECLARATION UNDER 37 C.F.R. § 1.132 of Richard A. Collins.

4. The purpose of this Declaration is to address the assertions in the Final Rejection that the application: (a) does not enable one skilled in

the art to make and/or use the invention; and (b) the claimed multiplex structure lacks patentable utility.

Enablement

5. Counsel for Ingeneus Corp. has advised me that an invention is patentably enabled if one of ordinary skill in the art could make or use the invention from the disclosures in the patent application coupled with information known in the art without undue experimentation. While I am not an expert in patent law, my experience and educational background, particularly as a professor of molecular biology and biochemistry, enable me to render an informed opinion as to the facts underlying the determination of enablement, including the level of ordinary skill in the art, information known in the art at the time of the invention, and what constitutes undue experimentation to one of ordinary skill in the art.

6. Composition claim 1 specifies a catalytic hybridization composition comprising a probe, an enzyme, a target and a hybridization medium, wherein at least one of the probe and the target is double-stranded and is bonded to the other of the probe or the target solely through Watson-Crick base triplets. Method claim 24 specifies a catalytic hybridization method for assaying binding, comprising the formation of probe-target multiplexes like those in claim 1. The meaning of Watson-Crick base triplets in the context of the invention is provided in the application at page 12, lines 17-22:

> In certain triplex and quadruplex embodiments, each nucleobase binds to no more than two other nucleobases. Thus, in addition to the traditional Watson-Crick base pairs, such embodiments include the following Watson-Crick base triplets: A-T-A, T-A-T, U-A-T, T-A-U, A-U-A, U-A-U, G-C-G and/or C-G-C (including C+-G-C, and/or any other ionized species of base).

in view of the following passage of the application at page 11, lines 17-24:

> As used herein, the term "Watson-Crick bonding" is intended to define specific association between opposing pairs of nucleic acid (and/or nucleic acid analogue) strands via matched, opposing bases. While the formation of a Watson-Crick quadruplex may sometimes be referred to as a hybridization event herein, that is merely for convenience and is not intended to limit the scope of the invention with respect to how the formation of a Watson-Crick quadruplex can be best characterized.

One of ordinary skill in the art would have understood from the foregoing that the probe-target multiplexes of claims 1 and 24 are triplexes of three nucleobase-containing strands and quadruplexes of four nucleobase-containing strands, wherein Adenines align with Thymines (or Uracils) and Cytosines align with Guanines.

7. Applicants have shown through binding studies specific association of non-denatured dsDNA targets with non-denatured dsDNA probes to form Watson-Crick multiplexes. The concentration of KCl used in, e.g., Example 1 of the parent application (09/664,827) was sufficiently high that it was highly unlikely that strand displacement occurred or that the dsDNA probes or dsDNA targets were denatured in any way. It is known that high concentrations of salt (e.g., 100 mM NaCl) inhibit strand invasion by virtue of the salt increasing the stability of dsDNA. See, e.g., Tomac et al., "Ionic Effects on the Stability and Conformation of Peptide Nucleic Acid Complexes," J. Am. Chem. Soc. 118, 5544-5552 (1996) (previously made of record in the application on January 18, 2002). Accordingly, one of ordinary skill in the art would have expected the 100 mM KCl concentration of Example 1 to prevent strand displacement and denaturation.

8. In light of Applicants' evidence that two strands on opposing non-denatured duplexes specifically interact together A:T(U) and C:G, one of

ordinary skill in the art would have found it reasonable to infer that adjacent bases in the remaining two strands of the duplexes would be brought into close enough proximity by the initial pairing of opposing strands to specifically interact together A:T(U) and C:G. This inference would not have been considered by an ordinarily skilled artisan to be unreasonable, particularly in view of the teachings of, e.g., Zhang et al., "Dimeric DNA Quadruplex Containing Major Groove Aligned A•T•A•T and G•C•G•C Tetrads Stabilized by Inter-subunit Watson-Crick A•T and G•C Pairs," 312 J. Mol. Biol. 1073-88 (Oct. 5, 2001), attached as Exhibit B.

9. Zhang et al. disproves the theory in the Final Rejection at page 6, last sentence, that "Watson-crick hydrogen bonding surfaces are inaccessible for any other strands [i.e., strands other than the two hybridized strands of conventional duplexes] since two strands are already interacting with each other at the center of the double helix." Zhang et al., shows through NMR studies the formation of A-T-A-T tetrads similar to previously discovered G-C-G-C tetrads. Zhang et al. at pages 1073-74 states:

> [E]fforts have been made to identify and characterize G•C•G•C tetrads, where a pair of Watson-Crick G•C pairs can potentially align either through their major groove or their minor groove edges. . . . recent studies have demonstrated that G•C•G•C tetrads aligned through their major groove edges can switch between two distinct alignment geometries [shown in Figure 1(a) and 1(b)]. . . . The major groove-aligned G•C•G•C tetrad has now been observed in a range of DNA quadruplexes and appears to be a robust tetrad motif adopted by a wide range of DNA sequences.

Figure 1 of Zhang et al. shows how major groove-aligned G•C•G•C and A•T•A•T tetrads in their direct alignment geometry have each G hydrogen bonded to each C, and each A hydrogen bonded to each T. Thus, contrary to the Final Rejection, Zhang et al. and the art cited therein shows that quadruplex G-C-G-C and A-T-A-T binding reasonably credible.

10. Thus, one of ordinary skill in the art (who has a high level of skill and a high tolerance for complex experimentation) would have been able to make and use with no more than routine experimentation compositions comprising Watson-Crick multiplexes for specific and useful purposes such as the catalytic hybridization assay of claim 24 without ever knowing for certain the location, length and/or number of hydrogen bonds between adjacent bases in the multiplex.

Utility

11. As shown by Zhang et al., the art recognizes the existence of quadruplex G-C-G-C and A-T-A-T binding under certain conditions, contrary to the assertion in the Final Rejection. Applicants have shown through binding studies specific association of non-denatured dsDNA targets with non-denatured dsDNA probes, wherein the targets and probes align Adenine to Thymine (or Uracil) and Cytosine to Guanine. Accordingly, one of ordinary skill in the art would have found the claimed invention to be reasonably credible in view of the original disclosure of the invention and conventional wisdom in the art.

12. Similarly, the binding studies described in the previously filed Daksis and Collins Declarations further show the reasonable credibility of the triplex embodiments of this invention, as do the inventors' previously issued U.S. Patents Nos. 6,420,115, 6,403,313 and 6,265,170, which include many examples of Watson-Crick triplex binding, wherein Adenines align with Thymines (or Uracils) and Cytosines align with Guanines.

13. In addition, I have personally observed triplex hybridization experiments similar to those described in the working examples of the application, wherein single-stranded probes were able to discriminate between

perfectly matched duplex targets and mismatched duplex targets under non-denaturing conditions. The experiments further convinced me of the high degree of recognition between the single-stranded probe and the duplex target with complete base pairing between binding partners.

I hereby declare that all statements made herein of my own knowledge are true, and that all statements made on information and belief are believed to be true; and further that these statements were made with the knowledge that willful false statements and the like so made are punishable by fine and/or imprisonment under Section 1001 of Title 18 of the United States Code, and that such willful false statements may jeopardize the validity of the application or any patent issuing therefrom.

Date: Sept 24, 2002

J. Hans van de Sande, Ph.D.

CURRICULUM VITAE

JOHAN H. van de SANDE

BIRTH DATE:		October 28, 1941
BIRTHPLACE:		Bergen op Zoom, Netherlands
NATIONALITY:		Canadian
DEGREES:	1963	B.Sc., University of Leiden Netherlands
	1968	Ph.D., Dept. of Chemistry, University of Alberta Edmonton, Alberta
AWARDS:	1959-1963	Dutch Government Scholarship
	1965-1968	National Research Council of Canada Studentship
	1967-1968	The University of Alberta Dissertation Fellowship
	1980-1981	Medical Research Council of Canada Visiting Professorship (Max Planck Institute, Goettingen, West Germany)
	1981	Alberta Heritage Foundation for Medical Research Visiting Scientist

PROFESSIONAL EXPERIENCE:

Post-doctoral Fellow	Institute for Enzyme Research, University of Wisconsin 1968-1970
Research Associate	Department of Biology, Massachusetts Institute of Technology 1970-1972
Assistant Professor	Division of Medical Biochemistry, The University of Calgary 1972-1975
Associate Professor	Division of Medical Biochemistry, The University of Calgary 1975-1979
Professor & Head	Department of Medical Biochemistry, The University of Calgary 1988-1993
Associate Dean (Research)	Faculty of Medicine, The University of Calgary 1993-1995
Professor	Department of Medical Biochemistry, The University of Calgary 1979-present
Director of Research	Alberta Cancer Board 1996 – 1998
Vice Dean	Faculty of Medicine, The University of Calgary 1998 - Present

INTRAMURAL ADMINISTRATIVE POSITIONS:

FACULTY:

Member	Executive Faculty Council (1973-1975, 1977-1979, 1993-1995)
Member	Curriculum Committee (1974-1977)
Chair	Space Allocation Committee (1973-1976)
Member	Research Committee (1979-1981, 1993-present)
Chair	Growth and Development Research Group (1973-1974, 1984-1985)
Member	Nominating Committee (1978-1979, l98l-l982,1985-1986) - (1990-1992)
Chair	Nominating Committee (1984-1985)
Member	Medical Student Admissions Committee (1982-1984)
Chair	Medical Student Admissions Committee (1985-1987)
Coordinator	Research Seminars (1973-1975)
Member	Budget Committee (1984-1986, 1993-present)
Chair	Student Appeals Committee (1987-1988)
Member	Research and Development Committee (1988-1992)
Member	Recruitment Priorities Committee (1992-1995)
Chair	DNA Synthesis Facility Committee (1982-present)
Member	Executive Committee, Partners in Health Campaign (1993-1995)
Chair	Planning and Priorities Committee (1998-present)
Member	Department Heads Selection Committees (1998-present)
Member	Chairs Selection Committees (1998-present)
Member	New Facility Planning Committee (1999 - present)

UNIVERSITY:

Member	University Space Allocations (1974-1976)
Member	Graduate Scholarship Committee (1974-1976)
Chair	Distinguished Lectures Series (1974-1978)
Member	University Biochemistry Group Executive (1980-1981, 1988-1990)
Member	Committee on Admissions and Transferability (1985-1987)
Member	Dean of Medicine Review (1987)
Member	Dean of Medicine Selection Committee (1991)
Member	University Bio NMR Users Committee (1987-1992)
Chair	University Bio NMR Users Committee (1992-1993)
Member	Appointment, Promotion and Dismissal Committee (1992-1993)
Member	Board of Governors (1993-1995)
Member	General Faculties Council (1993-1995)
Board Representative	Senate, University of Calgary (1993-1995)
Member	Calgary Research & Development Authority - Technical Advisory Committee (1993-1996)

EXTRAMURAL ADMINISTRATIVE POSITIONS:

Member	Medical Research Council of Canada Fellowship Committee (1975-1979)

Member	Medical Research Council of Canada Grants Panel (Molecular Biology) (1982-1983)
Chair	Medical Research Council of Canada Grants Panel (Molecular Biology) (1983-1988)
Member	Medical Research Council Biotechnology Training and Development Grants Panel (1983-1985)
Member	National Cancer Institute Grants Panel (1978-1982)
Member	Canadian Biochemical Society Nominating Committee (1974-1975)
Member	Provincial Cancer Hospitals Board Grants Committee (1980-1986)
Organizer	Northwest Nucleic Acids Conference (1973, 1976, 1980, 1988)
Member	Alberta Heritage Foundation for Medical Research - President Selection Advisory Committee (1990)
Member	Alberta Heritage Foundation for Medical Research Scholarship Renewal Committee (1988-1990)
Member	Human Frontier Science Molecular Biology Panel (1989-1991)
Vice-Chair	Program Advisory Committee - AHFMR (1991-1995)
Chair	Medical Research Council of Canada Program Grant Committee (1992-1994)
Member	Steacie Prize Awards Committee (1990-1991)
Member/Chair	MRC and University Site Visit Teams (1980-Present)
Regional Director	Medical Research Council (1994-1996)
Member	Council of Scientists - Human Frontier Science Program (1994-1997)
Member	Health Research Industry Task Force, Government of Alberta (1996)
Chair	Expert Review Panel - Protein Engineering Network of Centres of Excellence (PENCE) (1997)
Chair	Multidisciplinary Assessment Committee of the Canada Foundation for Innovation (1998-2000)
Member	Innovation and Science - Research Initiatives Program (2000)
Member	Gairdner Foundation (2000 – present)

EXTRAMURAL PROFESSIONAL ACTIVITIES:

Scientific Officer	Alberta Cancer Board (1986-1995, 1998-present)
Consultant	Du Pont PCR Litigation (1990-1992)
Consultant	BRL Lifetechnologies (1989-1991)
Consultant	Boehringer Mannheim (1985-1987)

TEACHING EXPERIENCE:

Biochemistry 549 (1974-1984) Independent Research Projects
Medicine 302 (1973-1980) Introductory Course (shared)
Medical Sciences 704 (1975-1980) Seminar Course Coordinator
Medical Sciences 601 (1975-1982) Cytology (shared)
Medical Sciences 642 (1974) Analysis of Development (shared)
Medical Sciences 823 (1982) Recombinant DNA Techniques course (shared)
Medical Sciences 613 (1983, 1985) Oncology (shared)

Nucleic Acids Graduate Course - Institute of Molecular & Cellular Biology - Singapore (1989,1991, 1994, 1996, 1998, 2000)

RESEARCH GRANTS:

Canadian Institute of Health Research Research – Structure, Function, & Properties of Uracil DNA glycosylase (1998-2001) $246,744

National Science and Engineering Research Council (1993-1999) $153,000.00

Canadian Institute of Health Research – Structure, Function, & Properties of Uracil DNA glycosylase (1993 – 1998) $496,242

Medical Research Council of Canada – Polynucleotide Conformation (1972 – 1992) $1,297,731

National Foundation March of Dimes (1977-1981) $110,000.00

Province of Alberta Cancer Hospitals Board (1979-1983) $120,000.00

Province of Alberta Cancer Hospitals Board - Equipment (1980-1981) $231,315.00

Alberta Heritage Foundation for Medical Research - Equipment (1981-1990) $415,000.00

NATO Collaborative Travel (1983-1986) $15,000.00

U.S. Biochemical Corporation (1991-1992) $17,500.00

Lifetechnologies (BRS) (1990-1992) $20,000.00

GRADUATE STUDENTS:

Shirley D. Semaka	Ph.D.	1977
Bernd W. Kalisch	M.Sc.	1978
John D. Sheppard	M.Sc	1978
George Chaconas	Ph.D.	1978
S. Wade Stoute	M.Sc.	1982
Freda D. Miller	Ph.D.	1985
Louise H. Naylor	Ph.D.	1987
Mark W. Germann	Ph.D.	1989
Priti Krishna	Ph.D.	1989
Fred Hagen	Ph.D.	1990
Harris Yee	M.Sc.	1991
Pallavi Devchand	Ph.D.	1994

POSTDOCTORAL FELLOWS:

Ken V. Deugau	1975-1978
K.H. Schoewaelder	1983-1985
H. Elzanowska	1983-1986
U. Varshney	1986-1988
K. Jorgensen	1987-1988
D. Creasey	1988-1991
P. Svendsen	1994-1998
M. Brown	1998-present

PUBLICATIONS

1. van de Sande, J.H. Studies in the oxidation of some olefins to allylic hydroperoxides. Ph.D. Thesis, The University of Alberta, pp. I-I95 (I968).

2. Kopecky, K.R., van de Sande, J.H. and Mumford, C. Preparation and base-catalyzed reactions of some -halohydroperoxides. Can. J. Chem. 46:25-34 (I968).

3. van de Sande, J.H. and Kopecky, K.R. Convenient C-alkylation of some acyloins. Can. J. Chem. 48:I63-I64 (I969).

4. Agarwal, K.L., Buchi, H., Caruthers, M.H., Gupta, N.H., Kleppe, K., Kornana, H.G., Kumar, A., Ohtsuka, E., RajBhandary, J.L., van de Sande, J.H., Sgaramella, V., Wever, H. and Yamada, T. The total synthesis of the gene for an alanine transfer ribonucleic acid from yeast. Nature 227:27-34 (I970).

5. Kleppe, K., van de Sande, J.H. and Khorana, H.G. Polynucleotide ligase-catalyzed joining of deoxyribo-oligonucleotides on ribopolynucleotide templates and of ribo-oligonucleotides on deoxyribonucleotide templates. Proc. Nat. Acad. Sci. USA 67:68-72 (I970).

6. Sgaramella, V., van de Sande, J.H. and Khorana, H.G. Studies on polynucleotides, C. A novel joining reaction catalyzed by the T4 polynucleotide ligase. Proc. Nat. Acad. Sci. USA 67:I468-I475 (I970).

7. Khorana, H.G., Agarwal, K.L., Buchi, H., Caruthers, M.H., Gupta, M.K., Kleppe, K., Kumar, A., Ohtsuka, E., RajBhandary, U.L., van de Sande, J.H. Sgaramella, V., Terao, T., Weber, H. and Yamada, T. Total synthesis of the structural gene for an alanine transfer ribonucleic acid from yeast. J. Mol. Biol. 72:209-2I7 (I972).

8. Caruthers, M.H., van de Sande, J.H. and Khorana, H.G. Total synthesis of the structural gene for an alanine transfer ribonucleic acid from yeast. Synthesis of three decadeoxynucleotides corresponding to the nucleotide sequence 5I-70. J. Mol. Biol. 72:375-405 (I972).

9. van de Sande, J.H., Caruthers, M.H., Sgaramella, V., Yamada, Y. and Khorana, H.G. Total synthesis of the structural gene for an alanine transfer ribonucleic acid from yeast. Enzymic joining of the chemically synthesized segments to form the DNA duplex corresponding to nucleotide sequence 46-77. J. Mol. Biol. 72:457 (I972).

10. Caruthers, M.H., Kleppe, K., van de Sande, J.H., Sgaramella, V., Agarwal, K.L., Buchi, H., Gupta, M.K., Kumar, A., Ohtsuka, E., RajBhandary, U.L., Terao, T., Wever, H., Yamada, T. and Khorana, H.G. Total synthesis of the structural gene for an alanine transfer ribonucleic acid from yeast. Enzymic joining to form the total DNA duplex. J. Mol. Biol. 72:475-492 (I972).

11. Besmer, P., Miller, R.C., Kumar, A., Minamoto, K., van de Sande, J.H., Siderova, M. and Khorana, H.G. Hybridization of polynucleotides with tyrosine transfer RNA sequences to the R-strand of o80PSU III. J. Mol. Biol. 72:502-522 (I972).

12. van de Sande, J.H., Loewen, P.C. and Khorana, H.G. A further study of ribonucleotide incorporation into deoxyribonucleotide chains by deoxyribonucleic acid polymerase I of Escherichia coli. J. Biol. Chem. 247:6140-6148 (1972).

13. Kopecky, K.R. and van de Sande, J.H. Deuterium isotope effects in the oxidation of 2,3-dimethyl-2-butene via the bromohydroperoxide, by singlet oxygen and by triphenyl phosphite ozonide. Can. J. Chem. 50:4034-4049 (1972).

14. Panet, A., van de Sande, J.H., Loewen, P.C., Raae, A.J., Lillehaug, J.L. and Kleppe, K. Physical characterization and simultaneous purification of polynucleotide kinase, polynucleotide ligase and DNA polymerase from E. coli infected with bacteriophage T4. Biochemistry 12:5045-5050 (1973).

15. van de Sande, J.H., Kleppe, K. and Khorana, H.G. Reversal of T4 bacteriophage induced polynucleotide kinase action. Biochemistry 12:5050-5055 (1973).

16. van de Sande, J.H. and Bilsker, M. Phosphorylation of N-protected deoxyoligonucleotides by T4 polynucleotide kinase. Biochemistry 12:5056-5062 (1973).

17. Powers, G.Y., Jones, R.L., Randall, G.A., Caruthers, M.H., van de Sande, J.H. and Khorana, H.G. Optimal strategies for the chemical and enzymatic synthesis of bihelical deoxyribonucleic acids. J. Am. Chem. Soc. 97:875-884 (1975).

18. Maniatis, T., Jeffrey, A. and van de Sande, J.H. Chain length determination of small double- and single-stranded DNA molecules by polyacrylamide gel electrophoresis. Biochemistry 14:3787-3794 (1975).

19. Imada, A., Hunt, J.W., van de Sande, J.H., Sinskey, A.J. and Tannenbaum, S.R. Purification and properties of an intracellular ribonuclease from Candida Lipolytica. Biochim. Biophys. Acta 395:490-500 (1975).

20. Lin, C.C., van de Sande, J.H., Smink, W.K. and Newton, D.R. Quinacrine fluorescence and Q-banding patterns of human chromosomes. Can. J. Genet. Cytol. 17:81-92 (1975).

21. Lin, C.C. and van de Sande, J.H. Differential fluorescent staining of human chromosomes by daunomycin and adriamycin - the D bands. Science 190:61-63 (1975).

22. Chaconas, G., van de Sande, J.H. and Church, R.B. Convenient methods to determine specific radioactivity of [_-32P]ATP. Anal. Biochem. 69:312-316 (1975).

23. Chaconas, G., van de Sande, J.H. and Church, R.B. End group labelling of RNA and double stranded DNA by phosphate exchange catalyzed by bacteriophage T4 induced polynucleotide kinase. Biochem. Biophys. Res. Comm. 66:962-969 (1975).

24. Khorana, H.G., Agarwal, K.L., Besmer, P., Buchi, H., Caruthers, M.H., Cashion, P., Fridkin, M., Jay, F., Kleppe, K., Kleppe, R., Kumar, A., Loewen, P.C., Miller, R.C., Minamoto, K., Panet, A., RajBhandary, U.L., RamaMoorthy, B., Sekiya, T., Takeya, T. and van de Sande, J.H. Total synthesis of the structural gene for the precursor of a tyrosine suppressor tRNA from E. coli I. General Introduction. J. Biol. Chem. 25l:565-570 (l976).

25. van de Sande, J.H., Caruthers, M.H., Kumar, A. and Khorana, H.G. Total synthesis of the structurals gene for the precursor of a tyrosine suppressor tRNA from E. coli. 2. Chemical synthesis of the deoxypolynucleotide segments corresponding to the nucleotide sequence l-3l. J. Biol. Chem. 25l:57l-586 (l976).

26. Minamoto, K., Caruthers, M.H., RamaMoorthy, B., van de Sande, J.H., Siderova, M. and Khorana, H.G. To synthesis of the structural gene for the precursor of a tyrosine suppressor of tRNA from E. coli. 3. Synthesis of deoxyribopolynucleotide segments corresponding to the nucleotide sequence 27-5l. J. Biol. Chem. 25l:587-598 (l976).

27. Agarwal, K.L., Caruthers, M.H., Fridkin, M., Kumar, A., van de Sande, J.H. and Khorana, H.G. Total synthesis of the structural gene for the precursor of a tyrosine supressor tRNA from E. coli. 4. Synthesis of deoxyribopolynucleotide segments corresponding to the nucleotide sequence 47-58. J. Biol. Chem. 25l: 599-608 (l976).

28. Agarwal, K.L., Caruthers, M.H., Buchi, H., van de Sande, J.H. and Khorana, H.G. Total synthesis of the structural gene for the precursor of a tyrosine suppressor tRNA from E. coli. 6. Synthesis of the deoxyribopolynucleotide segments corresponding to the nucleotide sequence l00-l26. J. Biol. Chem. 25l:624-64l (l976).

29. Kleppe, R., Sekiya, T., Loewen, P.C., Kleppe, K., Agarwal, K.L., Besmer, P., Buchi, H., Caruthers, M.H., Cahion, P., Fridkin, M., Jay, E., Kumar, A., Miller, R.C., Minamoto, K., Panet, A., RajBhandary, U.L., RamaMoorthy, B., Takeya, T., van de Sande, J.H. and Khorana, H.G. Total synthesis of the structural gene for the precursor of a tyrosine suppressor tRNA from E. coli. II. Enzymatic joining to form the total DNA duplex. J. Biol. Chem. 25l:667-675 (l976).

30. van de Sande, J.H. and Kalisch, B.W. Polymerization of oligodeoxythymidylates and oligoriboadenylates catalyzed by T4 polynucleotide ligase and their use as analytical markers in polyacrylamide gel electrophoresis. Anal. Biochem. 75: 509-52l (l976).

31. van de Sande, J.H., Lin, C.C. and Jorgenson, K.F. The reverse banding patterns (R-bands) on chromosomes produced by a G-C specific DNA binding antibiotic: olivomycin. Science l95:400-403 (l976).

32. van de Sande, J.H., Lin, C.C., Johnston, F.P. and Jorgenson, K.F. Differential fluorescent labelling of chromosomes and DNA with base pair specific. DNA binding antibiotics in Molecular cytogenetics - ICN-UCLA Symposium on Molecular and Cellular Biology, Vol. VI, pp. l27-l38 (l977).

33. Lin, C.C. and van de Sande, J.H. Mechanism of fluorescent banding in chromosomes: is base composition a primary determinant for the production of fluorescent bands? Bull. Gen. Soc. Can. 8:37-42 (l977).

34. van de Sande, J.H. and Lin, C.C. Differential fluorescent labelling of chromosomes and DNA with base pair specific DNA binding antibiotics. Journal of Supramolecular Structure. sup. 1, 105 (1977)

35. Johnston, F.P., van de Sande, J.H., Lin, C.C. and Jorgenson, K.F. Interaction of anthracyclines with DNA and chromosomes. Chromosoma 68:ll5-l29 (l978).

36. Deugau, K.V. and van de Sande, J.H. T4 polynucleotide ligase catalyzed joining of short DNA duplexes at base paired ends. Biochemistry l7:723-729 (l978).

37. Jorgenson, K.F., Lin, C.C. and van de Sande, J.H. Interaction of chromomycin-like antibiotics with DNA and chromosomes. Chromosoma 68:287-302 (l978).

38. Deugau, K.V., Lin, C.C. and van de Sande, J.H. Bisintercalating DNA binding ligands as chromosome banding agents. Exp. Cell Res. l20:439-444 (l978).

39. Shepherd, J.C., Fritzler, M.J., Watson, J.I. and van de Sande, J.H. A fluorescence assay for anti-double stranded DNA antibodies in Systemic Lupus Erythematosus. J. Rheumatology 5:39l-398 (l978).

40. van de Sande, J.H., Lin, C.C., and Deugau, D.V. Clearly Differentiated and Stable Chromosome Bands Produced by a Spermine Bis-acridine, a Bifunctional Intercalating Analogue of Quinarine. Exp. Cell Res. 120:439 (1979)

41. Kalisch, B.W. and van de Sande, J.H. The effect of antibiotics on T4 polynucleotide ligase catalyzed reactions. Nuc. Acids Res. 6:l88l-l894 (l979).

42. Loucks, E., Chaconas, G., Blakesley, R.B., Wells, R.D. and van de Sande, J.H. The effects of antibiotics on the electrophoretic mobility of DNA restriction fragments. Nuc. Acids Res. 6:l869-l880 (l979).

43. Davies, P.L., van de Sande, J.H. and Dixon, G.H. Determination of base composition of nanogram quantities of polynucleotides. Anal. Biochem. 93:26-30 (l980).

44. Chaconas, G. and van de Sande, J.H. 5'-32P-labelling of RNA and DNA restriction fragments. Meth. in Enzym., Vol. 65, pp. 75-85 (l980).

45. Lin, C.C., Jorgenson, K.F. and van de Sande, J.H. Specific fluorescent bands on chromosomes produced by acridine orange after prestaining with base specific non fluorescent DNA ligands. Chromosoma 79:27l-286 (l980).

46. Gedamu, L., Chaconas, G., van de Sande, J.H. and Dixon, G.H. Studies on the heterogeneity of the 5'-ends of the protamine mRNA's from rainbow trout testis. Bioscience Reports l:6l-70 (l98l).

47. Miller, F., Lin, C.C. and van de Sande, J.H. The interaction of DEAP fluoranthene with DNA and metaphase chromosomes. J. Histochem. and Cytochem. 29:969-978 (l98l).

48. van de Sande, J.H. and Jovin, T. Z* DNA, The left-handed helical form of poly1d(G-C)2 in MgCl2-ethanol is biologically active. EMBO Journal l:ll5-l20 (l982).

49. van de Sande, J.H., McIntosh, L.P. and Jovin, T.M. Mn++ and Other Transition Metals at Low Concentration Induce the Right-to-Left Helical Transformation of Poly d(G-C), EMBO 1:777-783 (1982).

50. Miller, F.D., Rattner, J.B. and van de Sande, J.H. Nucleosome core assembly on B and Z forms of poly d(G-m5C). Cold Spring Harb. Symp. Quant. Biol. 47:571-575 (1982).

51. Jovin, T.M., van de Sande, J.H., Zarling, D.A., Arndt-Jovin, D.J., Eckstein, F., Fuldner, H.H., Greider, C., Grieger, I., Kalisch, B.W., McIntosh, L.P., and Robert-Nicoud, M., (1982). Generation of left-handed Z DNA in solution and visualization in polytene chromosomes by immunofluorescence. Cold Spring Harb. Symp. Quant. Biol. 47:143-154 (1982).

52. McIntosh, L.P, Greiger, I., Eckstein, F., Zarling, D.A., van de Sande, J.H. and Jovin, T.M. The left-handed helical conformation of poly d(A-m5C)d(G-T). Nature 304:83-86 (l983).

53. Jovin, T.M., McIntosh, Arndt-Jovin, D.J., Zarling, D.A., Robert-Nicoud, M., van de Sande, J.H. Jorgenson, K.F. and Eckstein, F. Left-handed DNA: From synthetic polymers to chromosomes. J. Biomolec. Struct. Dyn. l:2l-57 (l983).

54. Stockton, J.F., Miller, F.D., Jorgenson, K.F., Zarling, D.A., Morgan, A.R., Rattner, J.B. and van de Sande, J.H. Left-handed Z-DNA regions are present in negatively supercoiled PM2 DNA. EMBO J. 2:2l23-2l28 (l983).

55. Miller, F.D., Jorgenson, K.F., Winkfein, R.J., van de Sande, J.H., Zarling, D.A., Stockton, J.F. and Rattner, J.B. Natural Occurrence of Left-handed regions in PM2 DNA. J. Biomolec. Struct. Dynam. l:6ll-620 (l983).

56. Jovin, T.M., McIntosh, L.P., Zarling, D.A., Arndt-Jovin, D.J., Robert-Nicoud, M., van de Sande, J.H. Probing for and with left-handed DNA: poly d(A-br5C).d(G-T), a member of a new family of Z-forming DNAs. in Pullman, B., (ed) Nucleic Acids: The Vectors of Life, D. Reidel, Dordrecht, Holland, pp. 89-99 (l983).

57. Hall, K., Cruz, P., Tinoco, I., Jovin, T.M. and van de Sande, J.H. Z-RNA: evidence for a left-handed RNA double helix. Nature 3ll:584-586 (1984).

58. Miller, F.D., Winkfein, R.J., Rattner, J.B. and van de Sande, J.H. Sequence analysis of a PM2 anti-Z IgG binding region. Bioscience Reports 4:885-895. (1984).

59. Miller, F.D., Rattner, J.B. and van de Sande, J.H. Assembly and characterization of nucleosome cores on B- versus Z-form DNA. Biochemistry 24:102-109 (1985).

60. Aiken, J., Miller, F.D., Hagen, F., McKenzie, D.I., Rattner, J.B., van de Sande, J.H. and Dixon, G.H. Characterization of a potential Z-DNA region adjacent to protamine genes in the Rainbow Trout. Biochemistry 24:6268-6276 (l985).

61. McIntosh, P.L., Jovin, T.M., Zielinski, J., Sprinzle, M., Kalisch, B.W. and van de Sande, J.H. Synthesis and characterization of poly d(G-Z5C) a 5' deoxyazacytidine containing polymer. Biochemistry 24: 4806-4814 (1985).

62. Germann, M.W., Schoenwaelder, K.H., van de Sande, J.H. Right- and left-handed helical (Z) conformations of the hairpin M(C-G)5T4(C-G)5 monomer and dimer. Biochemistry 24:4969-4973 (1985).

63. Kalisch, B.W., Krawetz, S.A., Schoenwaelder, K.H., van de Sande, J.H. Covalently linked sequencing primer linkers (splinkers) for sequence analysis of DNA restriction fragments. Gene 44:263-270 (1986).

64. Miller, F.D., Rattner, J.B. and van de Sande, J.H. Assembly of DNA onto the histone octamer facilitates the B- to Z-transition. Bioscience Reports 6: 467-476 (1986).

65. Naylor, L.H., Lilley, D.M.J. and van de Sande, J.H. Stress-induced cruciform formation in a cloned d(CATG)10 sequence. EMBO J. 5:2407-2413 (1986).

66. Krawetz, S.A., Kalish, B.W. and van de Sande, J.H. Covalently linked complementary oligodeoxynucleotides (splinkers) as tools for molecular biology. Nucl. Acids Res. 14:7131 (1986).

67. Naylor, L.H. and van de Sande, J.H. Improved sequence resolution of highly repetitive DNA fragments. Nucl. Acids Res. 14:5939 (1986).

68. van de Sande, J.H., Kalisch, B.W., Krawetz, S.A. and Schoewaelder, K.H. Covalently linked complementary oligodeoxynucleotides as universal nucleic acid sequencing primer linkers. U.S. Patent 801-900 (1986).

69. van de Sande, J.H., Naylor, L.H., Germann, M.W. and Yee, H. Conformational polymorphism in torsionnally stressed DNA in "Integration and Control of Metabolism Processes. ICSU and Cambridge Press (1987), p. 283-296.

70. Kubasek, W.L., Wang, Y., Thomas, G.A., Patupoff, T.W., Schoenwaelder, K.H., van de Sande, J.H. and Peticolas, W.L. Ramon Spectra of the model B-DNA oligomer d(CGCGAATTCGCG) and of the DNA in living salmon sperm show that they both have very similar B-type conformation. Biochemistry 25, 7440-7445 (1986).

71. Germann, M. and van de Sande, J.H. NACS-20 minor exchange chromatography of oligodeoyribonucleotides. Prediction of elution behaviours from length and sequence. Focus 9, 5-7 (1987).

72. Varshney, U. and van de Sande, J.H. Use of 32P-dNTPs to enhance the radioactive signal of 35S-dNTPs in Sanger's DNA sequence analysis. Biotechniques 5, 410-411 (1987).

73. Germann, M.W., Pon R. and van de Sande, J.H. A general method for the purification of synthetic oligodeoxynucleotides containing strong secondary structure by reversed phase. High performance liquid chromatography on PRP-1 resins. Anal. Biochem. 165, 399-405 (1987).

74. Naylor, L.H., Yee, H. and van de Sande, J.H. Length-dependent cruciform extension in d(GATC)n sequences. J. Biomol. Struct. Dynamics 5, 895-9l2 (1988).

75. Jorgenson, K.F., Varshney, U. and van de Sande, J.H. Interaction of Hoechst 33258 with repeating synthetic DNA polymers and natural DNA. J. Biomol. Struct. Dynamics, 5, 1005-1023 (1988).

76. Varshney, U., Jahroudi, N., van de Sande, J.H. and Gedamu, L. Inosine incorporation in GC rich RNA probes increases hybridization sequence specificity. Nucleic Acids Res. 16, 4162 (1988).

77. Antosiewicz, J., Germann, M.W., van de Sande, J.H. and Porschke, D. Helix-coil dynamics of a Z-helix hairpin. Biopolymers, 27, 1319-1327 (1988).

78. Varshney, U., Hutcheon, T. and van de Sande, J.H. Sequence analysis, expression and conservation of E. coli uracil DNA-glycosylase and it's gene (ung). J. Biol. Chem., 263, 7776-7784 (1988).

79. Wolk, S., Hardin, C.C., Germann, M.W., van de Sande, J.H. and Tinoco, T. Comparison of the B and Z-form hairpin loop structures formed by d(CG)5T4(CG)5. Biochemistry, 27, 5960-5967 (1988).

80. van de Sande, J.H., Ramsing, N., Germann, M.W., Elhorst, W., Kalisch, B.W., Pon, R.T. and Jovin, T.M. Parallel stranded DNA. Science, 241, 551-557 (l988).

81. Krishna, P., Kennedy, B.P., van de Sande, J.H. and McGhee, J.D. Yolk proteins from nematodes, chickens and frogs bind strongly and preferentially to left-handed Z-DNA. J. Biol. Chem., 263, 19066-19071 (1988).

82. Elzanowska, H. and van de Sande, J.H. Application of polarography to the study of complexation and stacking interactions of bases in the B-Z helical transition of poly[d(G-C)] and poly[d(G-m5C)] induced by Ni(II) and Mn(II). Bioelectrochemistry and Bioenergetics 19, 441-460 (1988).

83. Elzanowska, H. and van de Sande, J.H. Complexation of bases and phosphates of nucleic acid components by transition metal ions. Bioelectrochemistry and Bioenergetics 19, 425-439 (1988).

84. Germann, M.W., Kalisch, B.W. and van de Sande, J.H. Relative stability of Parallel and anti-parallel stranded DNA. Biochemistry 27, 8312-8316 (1988).

85. Varshney, U. and van de Sande, J.H. Characterization of the Ung1 mutation in E. coli. Nuc. Acids Res. 17, 813-814 (1989).

86. Germann, M.W., Vogel, H.J., Pon, R.T. and van de Sande, J.H. Characterization of a Parallel-Stranded DNA Hairpin. Biochemistry 28, 6220-6228 (1989).

87. Krishna, P., Kennedy, B.P., Waisman, W.D., van de Sande, J.H. and McGhee, J.D. Are many Z-DNA binding proteins actually phospholipid-binding Proteins? Proc. Nat. Acad. Sci. U.S.A. 87, 1292-1295 (1990).

88. Germann, M.W., Kalisch, B.W., Lundberg, P.,Vogel, H.J., and van de Sande, J.H. Perturbation of DNA hairpins containing the EcoRI recognition site by hairpin loops of varying size and composition: physical (NMR and UV) and enzymatic (EcoRI) studies. Nuc. Acids Res. 18, 1489-1498 (1990)

89. Germann, M.W., Kalisch, B.W., Pon, R.T. and J.H. van de Sande. Length Dependent formation of Parallel-Stranded DNA in Alternating A-T Segments. Biochemistry, 29, 9426-9432 (1990).

90. Wong, A.K.-C., Yee, H.A., van de Sande, J.H., and Rattner, J.B. Distribution of CT Rich Tracts Are Conserved in Vertebrate Chromosomes. Chromosoma, 99, 344-351 (1990).

91. Krishna, P., and van de Sande, J.H. Interaction of RecA Protein with Acidic phospholipids requires Ca++ or Mg++ and inhibits DNA binding activity of the protein. J. Bact. 172, 6452-6458 (1990).

92. van de Sande, J.H., Kalisch, B.W., Germann, M.W. Parallel-Stranded Nucleic Acids and Their Interaction with Intercalating and Groove Binding Drugs. In Pullman, B., (ed) Molecular Basis of Specificity in Nucleic Acid-Drug Interactions, Kluwer Academic Publ., Holland, p. 261-274 (1990).

93. Baleja, J.D., Germann, M.W., van de Sande, J.H. and B.D. Sykes. Solution conformation of purine-pyrimidine DNA octamers using nuclear magnetic resonance, restrained molecular dynamics and NOE-based refinement. J. Mol. Biol. 215, 411-428 (1990).

94. Krishna, P., Morgan, A.R. and van de Sande, J.H. Interaction of recA Protein with Left-Handed Z-DNA. Biochem. J. 275, 711-719 (1991).

95. Varshney, U., and van de Sande, J.H. Specificities and Kinetics of Uracil Excision from Uracil Containing Synthetic DNA Oligomers by E. coli uracil DNA glycosylase. Biochemistry, 30, 4055-4061 (1991).

96. H.A. Yee, A.K.C. Wong, J.H. van de Sande & J.B. Rattner. Identification of novel Single-Stranded $d(TC)_n$ Binding Proteins in Several Mammalian Species. Nucleic Acids Res. 19, 949-953 (1991).

97. Zhou, N., Germann, M.W., van de Sande, J.H., Pattabiraman, N. and Vogel, H.J. The solution structure of the parallel stranded hairpin d(T_8< >C_4A_8) as determined by two-dimensional N.M.R. Biochemistry 32(2), 646-656 (1993).

98. Krishna, P., Fritzler, M.J. and van de Sande, J.H. Interactions of Anti-DNA Antibodies with Z-DNA. Clinical & Experimental Immunology, Vol. 92 pp. 51-57 (1993).

99. Devchand, P., McGhee, J.D. and van de Sande, J.H. Uracil DNA glycosylase as a probe for protein-DNA interactions. Nucleic Acids Research, 21(15), 3437-3443 (1993).

100. Devchand, P.R., McGhee, J.D. van de Sande, J.H. Analysis of the Tet repressor-operator interactions using the uracil-DNA glycosylase footprinting system. Ann. N.Y. Acad. Sci., Vol. 726, 309-311 (1994).

101. Bryant, H., Brasher, P.M.A., van de Sande, J.H. and Turc, J.M. Review of methods in "Breast augmentation: a risk factor for breast cancer?" New Engl. J. Med. 330(4), 293 (1994).

102. Germann, M.W., Zhou, N., van de Sande, J.H. and Vogel, H.J. Parallel-stranded duplex DNA: an NMR perspective. Meth. in Enzym. 261, 207-225 (1995).

103. Maharaj, V., Tsankov, D., van de Sande, J.H. and H. Wieser. FT IR-VCD Spectra of Six Octadeoxynucleotides. J. Molec. Structure 349, 25-28 (1995).

104. Aramini, J.M., Kalisch, B.W., Pon, R.T., van de Sande, J.H. and Germann, M. Structure of a DNA Duplex That Contains -Anomeric Nucleotides and 3'-3' and 5'-5' Phosphodiester Linkages: Coexistence of Parallel and Antiparallel DNA. Biochemistry, Vol. 35, 9355-9365, (1996).

105. Germann, M.W., Kalisch, B.W. and van de Sande, J.H. Homooligomeric dA.dU and dA.dT Sequences in Parallel and Antiparallel Strand Orientation: Consequences of the 5-methyl Groups on Stability, Structure and Interaction with the Minor Groove Binding Drug HOECHST 33258. J. Biomolecular Structure & Dynamics, 13, 953-962, (1996).

106. Germann, M.W., Aramini J.M., Kalisch, B.W., Pon, R.T., and van de Sande, J.H. DNA Duplexes Containing alpha Anomeric Nucleotides and Polarity Reversals: Coexistence of Parallel and Antiparallel DNA. Nucleosides and Nucleotides, 17, 1481-1485 (1997).

107. Svendsen, P.C., Yee, H.A., Winkfein, R.J. and van de Sande, J.H. The mouse uracil-DNA glycosylase gene: Isolation of cDNA and genomic clones and mapping *ung* to mouse chromosome 5. GENE, 189, 175-181 (1997).

108. Aramini, J.M., van de Sande, J.H., and Germann, M.W. Spectroscopic and thermodynamic studies of DNA duplexes containing alpha anomeric C, A, and G nucleotides and polarity reversals: Coexistence of parallel and antiparallel DNA. Biochemistry, 36, 9715 - 9725 (1997).

109. Germann, M.W., Aramini, J.M., Kalisch, B.W. and van de Sande, J.H. (1997) Design and structural analysis of novel nucleic acid duplexes and mixed strand disposition. J. Biomol. Struct. & Dynamics 14, 790-791 (1997).

110. Tan, T.M.C., Kalisch, B.W., van de Sande, J.H. and Ting, R.C.Y. Effects of oligonucleotides with polarity and anomeric center reversal on cervical cells containing human papilloma virus type-16 DNA. Antisense and Drug Development, 8, 95-101 (1998).

111. Aramini, James A., van de Sande, J.H., and Germann, M.W. Structure and Stability of DNA Containing Inverted Anomeric Centers and Polarity Reversals in "Molecular Modeling of Nucleic Acids". ACS Symposium series 682, 92 - 105 (1998).

112. Germann, M.W., Kalisch, B.W., and van de Sande, J.H. (1998) Structure of d(GT)*n*.d(GA)*n* Sequences: Formation of Parallel Stranded Duplex DNA. Biochemistry 37, 12962-12970.

113. Kalish, B.W., Germann, M.W. and van de Sande, J.H. (1998) Antiparallel DNA Duplex Formation Between Alternating α d(GA)*n* and β d(GA)*n* Sequences. Federation of European Biochemical Societies 427, 301-304.

114. Germann, M.W., Kalish, B.W., van de Sande, J.H., NMR Spectroscopic and Enzymatic Studies of DNA Hairpins Containing Mismatches in the ECORI Recognition Site, Biochemistry and Cell Biology 76, 391-402 (1998).

115. V.V. Andrushchenko, J.H. van de Sande, and H. Wieser, 1998. Interaction of deoxyribonucleotides with devalent manganese ions: Comparison of vibrational circular dichroism and absorption spectroscopy. Vibrational Spectroscopy, 19 (2) (1999) pp.341-345.

116. V.V. Andrushchenko, J. H. van de Sande, H. Wieser, S.V. Kornilova, and Yu.P. Blagoi. Complexes of $(dG\text{-}dC)_{20}$ with Mn^{2+} ions: A study by Vibrational Circular Dichroism Spectroscopy. J. Biomol. Struct. & Dynamics, 17, 545-560, (1999).

117. Brown, M.L. and van de Sande, J.H. DNA Repair by Uracil DNA Glycosylase: Base Excision Repair from Bacteria to Man. Sappora Med J. 69 (Suppl.), 25-28 (2000).

118. V.V. Andrushchenko, J.L. McCann, J.H. van de Sande and H. Wieser. Determining structures of Polymeric Molecules by Vibrational Circular Dichroism (VCD) Spectroscopy. Vibrational Spectroscopy, 22, (2000) pp. 101-109.

119. M.W. Germann, J.M. Aramini, B.W. Kalish, and J.H. van de Sande. Structural, Dynamic and Enzymatic Properties of Mixed αβ-Oligonucleotides Containing Polarity Reversals. Nucleosides, Nucleotides and Nucleic Acids, 20:4:7: 493-499 (2001)

120. V.V. Andrushchenko, Z. Leonenko, D. Cramb, H. van de Sande and H. Weiser. Vibrational CD (VCD) and Atomic Force Microscopy (AFM) Study of DNA Interaction with Cr^{3+} Ions: VCD and AFM Evidence of DNA Condensation. Biopolymers, Vol 61, 243-260 (2002)

doi:10.1006/jmbi.2001.5002 available online at http://www.idealibrary.com on IDEAL J. Mol. Biol. (2001) 312, 1073–1088

JMB

Dimeric DNA Quadruplex Containing Major Groove-aligned A·T·A·T and G·C·G·C Tetrads Stabilized by Inter-subunit Watson-Crick A·T and G·C Pairs

Na Zhang†, Andrey Gorin†, Ananya Majumdar, Abdelali Kettani Natalya Chernichenko, Eugene Skripkin and Dinshaw J. Patel*

Cellular Biochemistry and Biophysics Program, Memorial Sloan-Kettering Cancer Center New York, NY 10021, USA

*Corresponding author

We report on an NMR study of unlabeled and uniformly ^{13}C,^{15}N-labeled d(GAGCAGGT) sequence in 1 M NaCl solution, conditions under which it forms a head-to-head dimeric quadruplex containing sequentially stacked G·C·G·C, G·G·G·G and A·T·A·T tetrads. We have identified, for the first time, a slipped A·T·A·T tetrad alignment, involving recognition of Watson-Crick A·T pairs along the major groove edges of opposing adenine residues. Strikingly, both Watson-Crick G·C and A·T pairings within the direct G·C·G·C and slipped A·T·A·T tetrads, respectively, occur between rather than within hairpin subunits of the dimeric d(GAGCAGGT) quadruplex. The hairpin turns in the head-to-head dimeric quadruplex involve single adenine residues and adds to our knowledge of chain reversal involving edgewise loops in DNA quadruplexes. Our structural studies, together with those from other laboratories, definitively establish that DNA quadruplex formation is not restricted to G_n repeat sequences, with their characteristic stacked uniform G·G·G·G tetrad architectures. Rather, the quadruplex fold is a more versatile and robust architecture, accessible to a range of mixed sequences, with the potential to facilitate G·C·G·C and A·T·A·T tetrad through major and minor groove alignment, in addition to G·G·G·G tetrad formation. The definitive experimental identification of such major groove-aligned mixed A·T·A·T and G·C·G·C tetrads within a quadruplex scaffold, has important implications for the potential alignment of duplex segments during homologous recombination.

Keywords: A·T·A·T and G·C·G·C tetrads; dimeric DNA quadruplex; hydrogen bond alignments; inter-subunit Watson-Crick pairs

Introduction

There is an increasing appreciation of the role DNA quadruplexes (reviews[1–4]) may play in biological processes ranging from replication, transcription and recombination (review[5]) to telomere function (review[4]). The earliest research focused on quadruplex formation involving stacked G·G·G·G tetrads (review[6]), with polymorphism introduced by the directionality of adjacent strands around the quadruplex (review[4]).

Formation of mixed tetrads could dramatically increase the versatility of quadruplex formation by allowing adoption of this four-stranded architecture by sequences other than simple G_n repeats. Towards this end, efforts have been made to identify and characterize G·C·G·C tetrads, where a pair of Watson-Crick G·C pairs can potentially align either through their major groove or their minor groove edges. This approach was successful in the case of the Fragile X syndrome triplet repeat-containing d(GCGGT$_3$GCGG) sequence, which dimerizes in solution through head-to-tail alignment of hairpins. The resulting quadruplex contains G·C·G·C tetrads, through major groove alignment of Watson-Crick G·C pairs (Figure 1(a)).[7]

†These authors contributed equally to the research.

Abbreviations used: NOE, nuclear Overhauser enhancement; NOESY, NOE spectroscopy; ppm, parts per million; HSQC, heteronuclear single quantum coherence; COSY, correlated spectroscopy; TOCSY, total COSY.

E-mail address of the corresponding author: pateld@mskcc.org

0022-2836/01/051073–16 $35.00/0

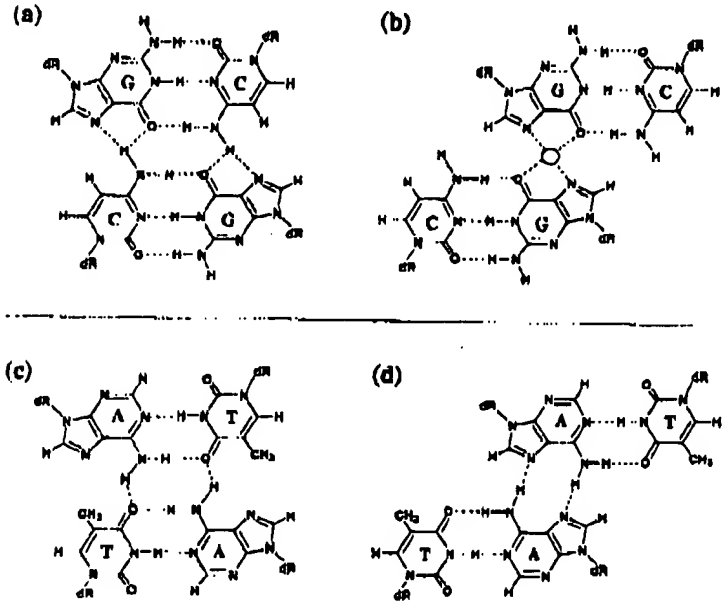

Figure 1. Potential G·C·G·C tetrad formation involving either (a) direct or (b) slipped alignment of major groove edges of a pair of Watson-Crick G·C pairs. The slipped alignment requires a monovalent cation to coordinate the inwardly oriented acceptor atoms. Potential A·T·A·T tetrad formation involving either (a) direct or (b) slipped alignment of major groove edges of a pair of Watson-Crick A·T pairs.

Independent structural studies have identified minor groove-aligned G·C·G·C tetrads (Supplementary Material, Figure S1(a)) in the crystalline[8] and solution states.[9]

More recent studies have demonstrated that G·C·G·C tetrads aligned through their major groove edges can switch between two distinct alignment geometries. In the direct alignment (Figure 1(a)), the two G·C pairs align directly opposite each other, resulting in the acceptor atoms (O6 and N7) of G pairing with the donor group (NH_2-4) of C. Alternately, in the slipped alignment (Figure 1(b)), the major groove edges of two guanine bases are positioned opposite each other. In this case, a monovalent cation (not necessarily in the plane of the tetrad) is needed to coordinate the four inwardly pointing nitrogen and oxygen acceptor atoms on the guanine bases (Figure 1(b)). Solution structural studies of the adeno associated viral repeat-containing d(GGGCT$_4$GGGC) sequence have demonstrated that the direct G·C·G·C tetrad alignment (Figure 1(a)) is formed in Na cation solution,[10] while the slipped G·C·G·C tetrad alignment (Figure 1(b)) is formed in K cation solution.[11] Such conformational transitions were unanticipated, and attest to the diversity of pairing geometries in mixed tetrad alignments and the role of cations in modulating this transition.

The major groove-aligned G·C·G·C tetrad has now been observed in a range of DNA quadruplexes[7,10,12] and appears to be a robust tetrad motif adopted by a range of DNA sequences. One can therefore anticipate potential formati n of the corresponding major-groove aligned A·T·A·T counterpart, either of the direct (Figure 1(c)) or slipped (Figure 1(d)) alignment type. By contrast, the corresponding minor groove-aligned A·T·A·T tetrad, of the slipped cation-coordination type (Supplementary Material, Figure S1(b)), has been reported earlier both in the crystalline[13] and solution[9] states.

Demonstration of the major groove-aligned A·T·A·T tetrad formation has turned out to be a considerable challenge, and after many unsuccessful attempts, our group has now identified a sequence, d(GAGCAGGT), which forms a head-to-head dimeric quadruplex (Figure 2a and Supplementary Material, Figure S2), stabilized by direct G·C·G·C (Figure 2(b)) and slipped A·T·A·T (Figure 2(d)) tetrads, flanking a central G·G·G·G tetrad (Figure 2(c)). Strikingly, we observe Watson-Crick G·C pairing between monomer subunits within the G·C·G·C tetrad and Watson-Crick A·T pairing between monomer subunits within the A·T·A·T tetrad in this quadruplex. Finally, the edgewise turns in the head-to-head dimeric quadruplex involve a single adenine residue and provide new insights into chain reversal in DNA quadruplexes.

Results

Our group scanned a range of sequences containing G, A and T residues in our attempts to generate a major groove-aligned A·T·A·T tetrad, stabilized through stacking on a G·G·G·G tetrad within a quadruplex scaffold. This approach has worked in the past in our laboratory when we have generated stable triads[15-18] and A·(G·G·G·G)·A hexads,[12,19] stabilized through stacking on G·G·G·G tetrads within a quadruplex

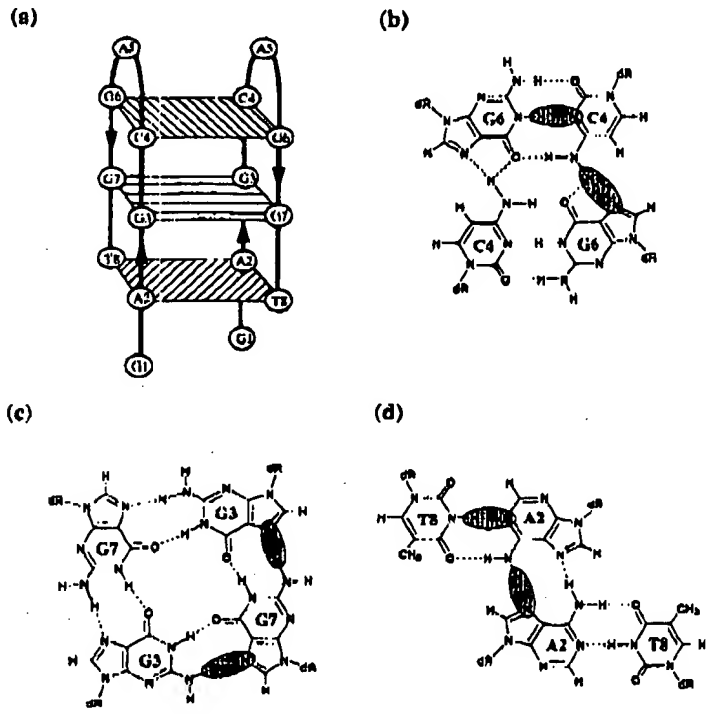

Figure 2. (a) Folding topology of a head-to-head dimeric d(GAGCAGGT) quadruplex in 1 M NaCl. The backbone tracing of the individual strands are shown by thick lines and the chain directionality indicated by arrows. Pairing alignments for (b) the G6·C4·G6·C4 tetrad, (c) the G3·G7·G3·G7 tetrad and (d) the A2·T8·A2·T8 tetrad.

scaffold. We report on NMR studies of the d(GAGCAGGT) sequence, which forms a dimeric quadruplex containing a major groove-aligned slipped A·T·A·T (Figure 2(c)) tetrad.

Imino proton spectra and assignments

The exchangeable proton spectrum (5.5 to 14.5 ppm) of the d(GAGCAGGT) sequence was highly dependent on added NaCl concentration. At low NaCl concentration, the predominant conformation gave very broad resonances in slow exchange with a minor component that gave narrow resonances (Supplementary Material, Figure S3). The equilibrium shifted with increasing NaCl to the conformation that exhibited narrow resonances, resulting in the spectrum shown in Figure 3(a) in 1 M NaCl, 2 mM phosphate buffer (pH 6.6) at 10 °C. This spectrum exhibits well resolved exchangeable (8.0 to 15.0 ppm) and non-exchangeable (7.0 to 8.7 ppm) resonances, with the total number of imino, amino and base proton resonances consistent with formation of a single conformer in solution. We observe two narrow imino protons between 11 and 12 ppm, a region characteristic of N-H···O hydrogen bonds,[4] and narrow resonances at 13.11 ppm and 14.28 ppm, a region characteristic of N-H···N hydrogen bonds[4] (Figure 3(a)). We also observe two narrow amino proton resonances between 8.0 and 8.5 ppm and two additional narrow amino proton resonances downfield-shifted between 9.0 and 9.2 ppm (Figure 3(a)).

The exchangeable imino and amino protons have been assigned following analysis of two-dimensional data sets on unlabeled and uniformly ^{13}C,^{15}N-labeled d(GAGCAGGT) sequence. An expanded 60 ms mixing time NOESY contour plot of d(GAGCAGGT) in 1 M NaCl at 0 °C is plotted in Figure 3(b). The NOE cross-peaks are labeled in the Figure and the assignments are given in the legend. The corresponding NOESY data set recorded at a longer mixing time of 200 ms is plotted in Supplementary Material, Figure S4, and the cross-peaks assignments listed in the legend. We could readily distinguish thymine from guanine imino protons because of their distinct nitrogen chemical shifts in a ^{1}H-^{15}N HSQC spectrum (Supplementary Material, Figure S5).

We establish formation of an A2·T8 Watson-Crick base-pair based on NOEs between the imino proton of T8 and the amino (peaks a and a', Figure 3(b)) and H2 (peak b, Figure 3(b)) protons of A2. In addition, we unexpectedly observe NOEs between the H8 and NH_2 protons of A2 (peaks n and n', Figure 3(b)), consistent with formation of a major groove-aligned slipped A2·T8·A2·T8 tetrad, schematically outlined in Figure 2(d).

We establish formation of a G6·C4 Watson-Crick base-pair based on NOEs between the imino proton of G6 and the amino protons of C4 (peaks c

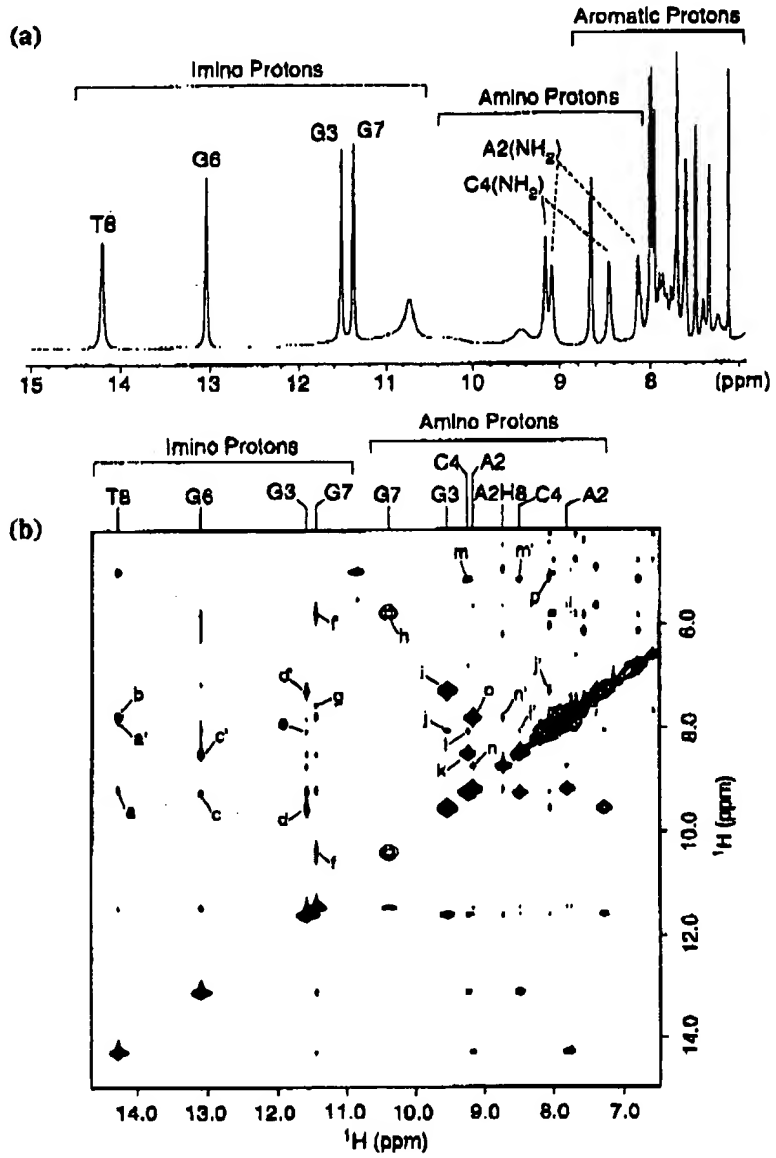

Figure 3. (a) Proton NMR spectrum (7.0 to 15.0 ppm) of the d(GAGCAGGT) quadruplex (8.8 mM in strands) in 1 M NaCl, 2 mM phosphate in H_2O (pH 6.6) at 10°C. (b) Expanded NOESY (60 ms mixing time) contour plot correlating NOEs between imino, amino and non-exchangeable protons in the d(GAGCAGGT) quadruplex in 1 M NaCl, 2 mM phosphate, H_2O (pH 6.6) at 0°C. The NOE cross-peaks a to p are assigned as follows: a and a', T8(NH3)-A2(NH_2-6); b, T8(NH3)-A2(H2); c and c', G6(NH1)-C4(NH_2-4); d and d', G3(NH1)-G3(NH_2-2); e, G3(NH1)-G7(H8); f and f', G7(NH1)-G7(NH_2-2); g (observable in 200 ms mixing time NOESY experiment), G7(NH1)-G3(H8); h, G7(NH_2-2)-G7(NH_2-2); i, G3(NH_2-2)-G3(NH_2-2); j and j', G3(NH_2-2)-G7(H8); k, C4(NH_2-4)-C4(NH_2-4); l and l', C4(NH_2-4)-G6(H8); m and m', C4(NH_2-4)-C4(H5); n and n', A2(NH_2-6)-A2(H8); o, A2(NH_2-6)-A2(NH_2-6); p, G6(H8)-C4(H5).

and c', Figure 3(b)). We also detect NOEs between the amino protons of C4 and the H8 proton of G6 (peaks l and l', Figure 3(b)), and between the H5 proton of C4 and the H8 proton of G6 (peak p, Figure 3(b)), consistent with formation of a major groove-aligned direct G6·C4·G6·C4 tetrad, schematically outlined in Figure 2(b).

The narrow G3 and G7 imino protons exhibit a set of NOEs indicative of G3·G7·G3·G7 tetrad formation, schematically outlined in Figure 2(c).

These include NOEs between the H8 proton of G7 with the imino (peak e, Figure 3(b)) and amino (peak j and j', Figure 3(b)) protons of G3, and an NOE between the H8 proton of G3 and the imino proton of G7 (box g, Figure 3(b); observable in 200 ms NOESY spectrum, peak g, Supplementary Material, Figure S4).

The NOE data outlined above for the d(GAGCAGGT) sequence are consistent with formation of slipped A2·T8·A2·T8 (Figure 2(d)), direct G6·C4·G6·C4 (Figure 2(b)) and G3·G7·G3·G7 (Figure 2c) tetrads. This can be most readily achieved by head-to-head dimerization to form a quadruplex as shown schematically in Figure 2(a) and Supplementary Material, Figure S2. The exchangeable imino and amino proton chemical shifts of the d(GAGCAGGT) quadruplex are listed in Supplementary Material, Table S1.

Non-exchangeable proton spectra and assignments

The non-exchangeable base and sugar protons have been assigned following analysis of two-dimensional data sets on unlabeled and uniformly ^{13}C,^{15}N-labeled d(GAGCAGGT) sequence. An expanded 250 ms mixing time NOESY contour plot of d(GAGCAGGT) quadruplex in 1 M NaCl, ^2H_2O buffer at 10 °C is plotted in Figure 4(a), along with a tracing of distance connectivities between base protons and their own and 5'-flanking sugar H1' protons from G1 to T8 in the sequence. The G3 residue adops a *syn* alignment based on the strong H8 to its own H1' NOE in a 50 ms mixing NOESY stacked plot (Figure 4(b)). The remaining sugar proton chemical shifts were obtained from an analysis of other regions of the through space NOESY contour plot and through bond COSY and TOCSY correlations of the assigned sugar H1' protons with the remaining sugar protons within individual rings. The non-exchangeable base and sugar proton chemical shifts of the d(GAGCAGGT) quadruplex are listed in Supplementary Material, Table S2. The H8 proton of A2 (8.71 ppm) is downfield-shifted while the H6 (6.78 ppm) and H5 (5.15 ppm) protons of C4 are somewhat upfield-shifted.

We can also correlate exchangeable imino protons with their own H8 protons within individual guanine bases, *via* through bond correlations to their C5 ring carbon atoms.[20] Such a correlation experiment on the sample of uniformly ^{13}C,^{15}N-labeled d(GAGCAGGT) sequence is shown in Figure 4(c).

Hydrogen bond alignments

We have verified the formation of NOE-based G6·C4·G6·C4 (Figure 2(b)), G3·G7·G3·G7 (Figure 2(c)) and A2·T8·A2·T8 (Figure 2(d)) tetrad alignments, by identifying through bond coupling connectivities across N-H··N hydrogen bonds[21–25] within the folded architecture of the uniformly ^{13}C,^{15}N-labeled d(GAGCAGGT) quadruplex in 1 M NaCl, H_2O buffer at 0 °C. The amino protons of A2, G3 and C4 could be correlated with their directly attached nitrogen atoms using this labeled sample as shown in Supplementary Material, Figure S6.

We observe a N-H··N hydrogen bond connectivity between the N1H donor of G6 and the N3 acceptor of C4 (peak 4, Figure 5(a)) in a HNN-COSY experiment[24] recorded on the d(GAGCAGGT) quadruplex. This connectivity provides direct support for a Watson-Crick G6·C4 alignment (observed couplings as shaded region in Figure 2(b)). In addition, we observe HNN-COSY coupling connectivities between the NH_2 protons of C4 and the N7 of G6 (peaks 1 and 1', Figure 5(b)) and four bond H(CN)N(H) coupling connectivities[24] between the N4 of C4 and the H8 of G6 (peak 3, Figure 5(c)). These observations verify the direct alignment of opposing Watson-Crick G6·C4 pairs through their major groove edges (observed coupling as shaded region in Figure 2(b)), to form the G6·C4·G6·C4 tetrad outlined in Figure 2(b).

The observed H(CN)N(H) coupling connectivities[24] between the H8 proton of G7 and the N2 of G3 (peak 1, Figure 5(c)) and between the H8 proton of G3 and the N2 of G7 (peak 2, Figure 5(c)), verify the proposed hydrogen bonding patterns (shaded regions in Figure 2(c)) around the G3·G7·G3·G7 tetrad.

We observe a N-H··N hydrogen bond connectivity between the N3H donor of T8 and the N1 acceptor of A2 (peak 2, Figure 5(a)) in a HNN-COSY experiment. This connectivity provides direct support for a Watson-Crick A2·T8 alignment. In addition, we observe HNN-COSY coupling connectivities between the NH_2 protons of A2 and the N7 of A2 (peaks 2 and 2', Figure 5(b)). This connectivity could be either within an adenine or between adenine bases positioned opposite each other and hydrogen-bonded through their major groove edges, as shown for the A2·T8·A2·T8 tetrad alignment in Figure 2(d). We do not observe the corresponding coupling connectivities between the NH_2 and N7 of A5, and hence we favor the latter explanation over the former. These observations verify the slipped alignment of opposing Watson-Crick A2·T8 pairs through their major groove edges, to form the A2·T8·A2·T8 tetrad outlined in Figure 2(d).

Intra-strand *versus* inter-strand NOE restraints

The 2-fold symmetry in the dimeric d(GAGCAGGT) quadruplex fold makes it critical to unambiguously differentiate between intra-strand and inter-strand contributions for key NOEs that define the folding topology in solution. We prepared a sample containing an equimolar mixture of unlabeled and uniformly ^{13}C,^{15}N-labeled d(GAGCAGGT) sequences and recorded ^{15}N-edited (ω_1), ^{13}C,^{15}N-purged (ω_2) NOESY[26] (100 ms mixing time) spectra in 1 M NaCl-containing H_2O

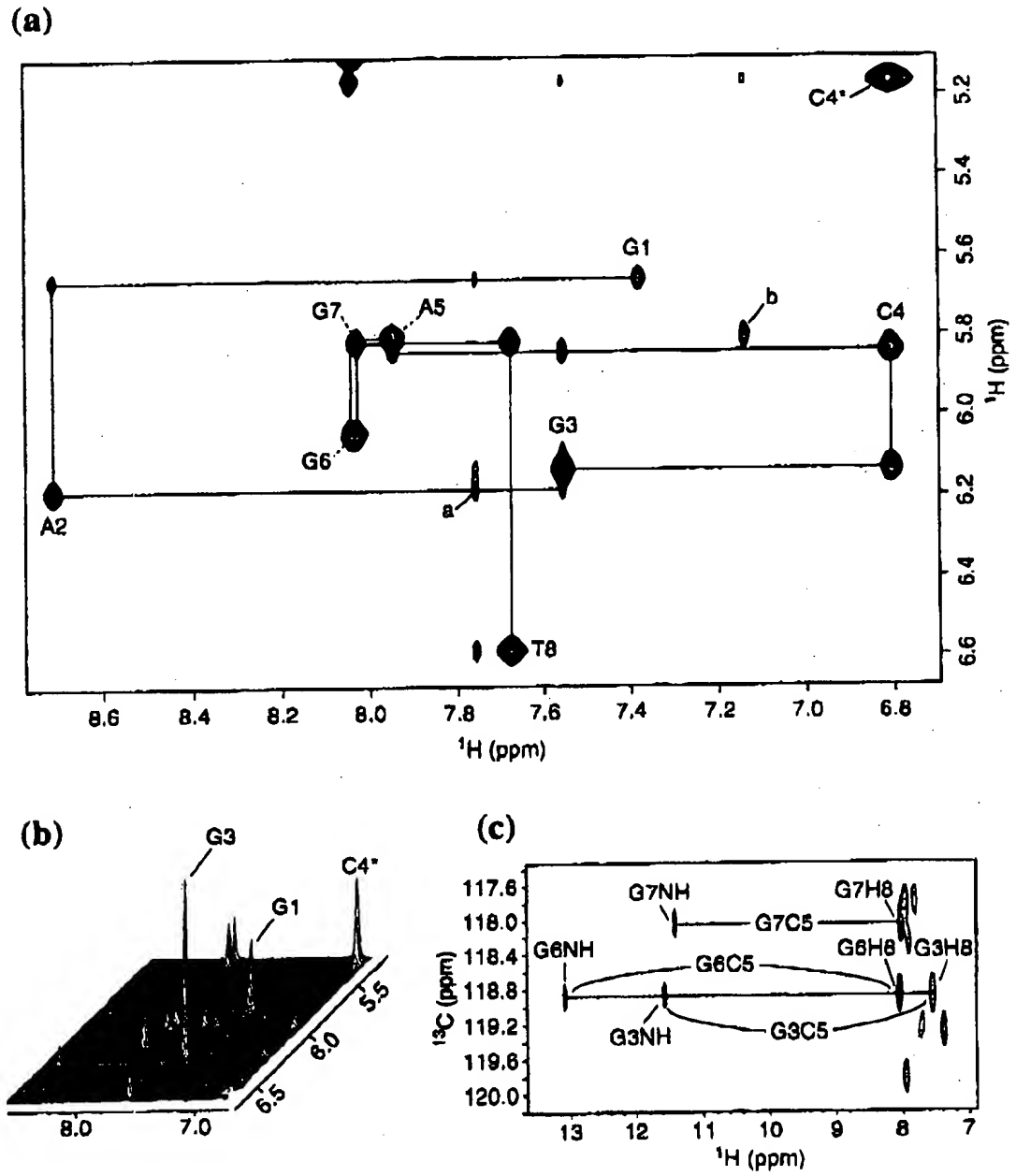

Figure 4. (a) Expanded NOESY (250 ms mixing time) contour plot correlating NOEs between base and sugar H-1′ protons in the d(GAGCAGGT) quadruplex (8.8 mM in strands) in 1 M NaCl, 2 mM phosphate, ^2H_2O (pH 6.6) at 10 °C. The cytidine H6 and H5 NOEs are designated by asterisks. The NOE cross-peaks a and b are assigned as follows: a, A2(H2)-A2(H1′); b, A5(H2)-A5(H1′). (b) Expanded NOESY (50 ms mixing time) stacked plot correlating NOEs between base and sugar H-1′ protons in the d(GAGCAGGT) quadruplex (8.8 mM in strands) in 1 M NaCl, 2 mM phosphate, ^2H_2O (pH 6.6) at 0 °C. The cytidine H6 and H5 NOEs are designated by asterisks. (c) Correlation of the guanine imino and H8 protons by through-bond connectivities to the C5 carbon within individual guanine rings in the uniformly ^{13}C,^{15}N-labled d(GAGCAGGT) quadruplex (5.3 mM in strands) in 1 M NaCl, 2 mM phosphate, ^2H_2O (pH 6.6) at 0 °C.

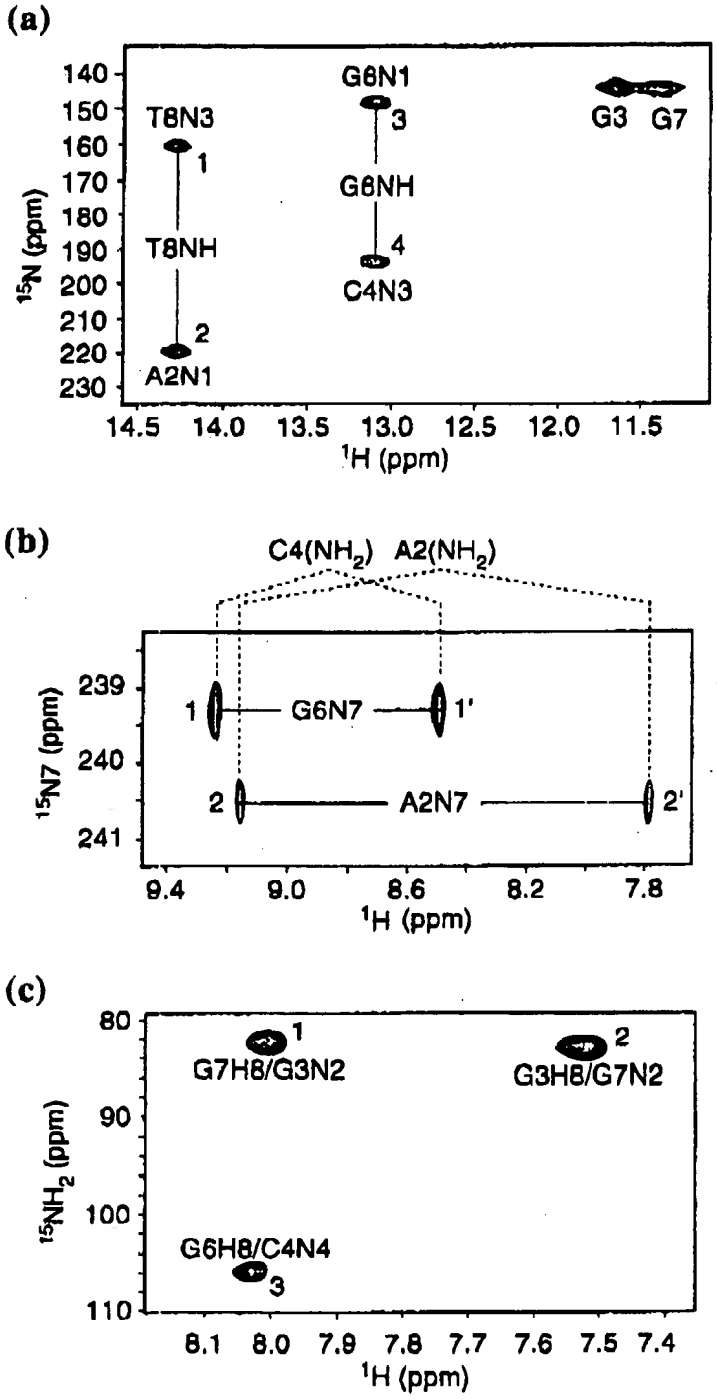

Figure 5. Identification of N-H··N hydrogen bond alignments in uniformly ^{13}C, ^{15}N-labeled d(GAGCAGGT) (5.3 mM in strands) in 1 M NaCl, 2 mM phosphate, H_2O (pH 6.6) at 0°C. Expanded $^{2h}J_{NN}$ HNN-COSY contour plots correlating two-bond coupling connectivities between donor and acceptor nitrogen atoms within N-H··N hydrogen-bond alignments across base-pairs. (a) Two-bond coupling connectivities between T8(N3) imino donor and A2(N1) acceptor nitrogen atoms (peak 2) across the A2(N1)·T8(N3 donor) Watson-Crick base-pair and between G6(N1) imino donor and C4(N3) acceptor nitrogen atoms (peak 4) across the C4(N3)·G6(N1 donor) Watson-Crick base-pair. (b) Two-bond coupling connectivities between C4(N4) amino donor and G6(N7) acceptor nitrogen atoms (peaks 1,1') across C4(N4 amino)·G6(N7) mismatch pair and between A2(N6) amino donor and A2(N7) acceptor nitrogen atoms (peaks 2,2') across A2(N6 amino)·A2(N7) mismatch pair. (c) H(CN)N(H) spectrum showing inter-nucleotide H8(ω_3)-N2(ω_1) and H8(ω_2)-N4(ω_1) cross-peaks. The spectrum consisted of 608 (t_2) * 60 (t_1) complex points, with 160 transients per FID. Spectral widths of 2000 Hz ($t_1$max: 30 ms) and 8000 Hz ($t_2$max: 76 ms) were used, with a relaxation delay of two seconds, resulting in a total acquisition of 12 hours. Coupling connectivities are observed between the H8 of G7 and the N2 of G3 (peak 1), between the H8 of G3 and the N2 of G7 (peak 2), as well as between the H8 of G6 and N4 of C4 (peak 3). A coupling connectivity was not detectable between the H8 of A2 and the N6 of A2.

buffer solution at 0°C, to identify inter-strand NOEs and differentiate them from their intra-strand counterparts, for the 50% component in the mixture where the quadruplex contains one unlabeled and one uniformly labeled strand. We observe inter-strand NOEs between the imino pro-

ton of T8 and the amino (peaks 1 and 1', Figure 6(a); peaks 1 and 1', Figure 6(b)) and H2 (peak 2, Figure 6(b)) protons of A2, establishing formation of Watson-Crick A2·T8 pairs between hairpin subunits in the dimeric d(GAGCAGGT) quadruplex. We also observe inter-strand NOEs between the imino proton of G6 and the amino protons of C4 (peaks 2 and 2', Figure 6(a); peaks 3 and 3', Figure 6(b)), establishing formation of Watson-Crick G6·C4 pairs between hairpin subunits in the dimeric d(GAGCAGGT) quadruplex.

We also observe inter-strand NOEs between the amino protons of A2 and the H8 proton of A2 (peaks 4 and 4', Figure 6(a)), putting restraints on the relative alignments of the A·T base-pairs around the A·T·A·T tetrad. Interstrand NOEs are also observed between the imino proton of G7 and the H2 proton of A2 (peak 4, Figure 6(b)), putting restraints on the relative stacking of adjacent G3·G7·G3·G7 and A2·T8·A2·T8 tetrads in the quadruplex.

Distance restraints and molecular dynamics calculations

Distance restraints associated with exchangeable protons (total of 115) were qualitatively deduced from NOESY experiments in H_2O at two mixing times, while those associated with their non-exchangeable proton counterparts (total of 178) were quantified from NOE buildup curves in ^2H_2O at four mixing times, as outlined in Materials and Methods. The observation of a single set of narrow resonances for the d(GAGCAGGT) sequence at temperatures down to 0 °C, was consistent with formation of a dimeric quadruplex, containing two strands related by a 2-fold symmetry axis. Therefore, non-crystallographic symmetry restraints were used during the computations. All distance restraints were classified as ambiguous during the distance-restrained molecular dynamics computations. Experimentally defined hydrogen bonding alignments from NOE patterns on unlabeled sample, N-H··N scalar couplings on isotopically labeled sample, and intermolecular NOEs on an equimolar mixture of labeled and unlabeled sample, were used to restrain the G6·C4·G6·C4 (Figure 2(b)), G3·G7·G3·G7 (Figure 2(c)) and A2·T8·A2·T8 (Figure 2(d)) tetrads, with the folding models retaining these hydrogen bonding alignments during the computations.

The solution structure of the dimeric d(GAGCAGGT) quadruplex in 1 M NaCl was solved by molecular dynamics computations guided by hydrogen bonding and NOE distance restraints. Sixty starting structures were generated for the d(GAGCAGGT) 8-mer segment as sets of pairs of randomized chains separated by space intervals of 50 Å. The protocol outlined in Materials and Methods involved initial torsion space dynamics at 20,000 K followed by Cartesian space dynamics at 300 K. A subset of ten distance-refined structures of the d(GAGCAGGT) quadruplex were identified based on a combination of low NOE energies and fewest NOE violations.

Intensity restraints and NOE back calculations

The subset of ten converged distance-refined structures were next refined against the non-exchangeable proton NOE intensities associated with NOESY spectra recorded at four mixing times. These computations utilized a molecular dynamics with back calculation protocol outlined in Materials and Methods. The NOE violations, deviations from covalent geometry and pairwise r.m.s.d. values for the ten lowest energy intensity-refined structures of the d(GAGCAGGT) quadruplex (less the poorly defined G1 residues) are listed in Table 1.

Structural features

A stereo view of the ten superpositioned lowest energy intensity refined structures of the d(GAGCAGGT) quadruplex (less the poorly defined G1 residues) is shown in Figure 7(a). The sugar-phosphate backbone of individual symmetry-related hairpins are colored in orange and green, with the sequentially stacked loop A5 residue, G6·C4·G6·C4 tetrad, G3·G7·G3·G7 tetrad and A2·T8·A2·T8 tetrad colored in white, magenta, yellow and cyan, respectively. Ribbon and surface views of one representative refined structure of the d(GAGCAGGT) quadruplex using the GRASP program are plotted in Figure 7(b) and (c), respectively.

A stick representation of one symmetric strand of the d(GAGCAGGT) quadruplex (less the poorly defined G1 residues) is shown in Figure 8(a). The pairing alignments of the G6·C4·G6·C4 tetrad and A2·T8·A2·T8 tetrad in this representative structure are shown in Figure 8(b) and (c), respectively.

The stacking geometries between the A5 bases (in white) with the G6·C4·G6·C4 tetrad (in magenta) is shown in Figure 9(a), while that between the G6·C4·G6·C4 tetrad (in magenta) and the G3·G7·G3·G7 tetrad (in yellow) is shown in Figure 9(b). The overlap geometry between the G3·G7·G3·G7 tetrad (in yellow) and the A2·T8·A2·T8 tetrad (in cyan) is shown in Figure 9(c).

Discussion

The NMR-based structural characterization of the d(GAGCAGGT) quadruplex was considerably aided by the narrow and well-resolved resonances of the one and two-dimensional proton NMR spectra, and the availability of uniformly ^{13}C, ^{15}N-labeled sequence, which aided greatly in the resonance assignment and identification of hydrogen bonding alignments. The computations were also aided by our ability to distinguish between inter-strand and intra-strand NOEs (and in turn, Watson-Crick hydrogen bonding alignments) using

Table 1. NMR restraints and structural statistics for the intensity refined structures of the dimeric d(GAGCAGGT) quadruplex

	Non-exchangeable	Exchangeable
A. *NMR restraints*		
Distance restraints[a]	86	19
Intra-residue distance restraints	76	45
Sequential (i, $i+1$) distance restraints	16	51
Long range $\geq (i, i+2)$ distance restraints		
Other restraints		
Hydrogen bonding restraints[b]	48	
Torsion angle restraints[c]	14	
Intensity restraints[a]		
Non-exchangeable protons (each of 4 mixing times)	178	
B. *Structural statistics in complex following intensity refinement*		
NOE violations		
Number >0.2 Å	6.1±0.7	
Maximum violations	0.27±0.03	
r.m.s.d. of violations	0.056±0.02	
NMR R factor ($R_{1/6}$)	0.074±0.003	
Deviations from ideal covalent geometry		
Bond lengths	0.011±0.001	
Bond angles	3.70±0.09	
Impropers	0.40±0.03	
Pairwise all heavy atom r.m.s.d. values (10 refined strucutres)		
All heavy atoms excluding G1	0.78±0.17	

[a] All distance restraints were set as ambiguous between intra and inter-residue contributions.
[b] These hydrogen bonding restraints are based on experimental NOE and $^3J_{NN}$ coupling data.
[c] Residues A2, C4, A5, G6, G7 and T8 were restrained to χ values in the 210(±40)° range, characteristic of *anti* glycosidic torsion angles, while residues G3 were restrained to χ values in the 65(±40)° range, characteristic of *syn* glycosidic torsion angles, identified experimentally.

equimolar mixtures of labeled and unlabeled samples of the quadruplex.

Quadruplex architecture

The experimental data on the d(GAGCAGGT) sequence is consistent with formation a dimeric quadruplex in 1 M NaCl solution. Individual strands of d(GAGCAGGT) form hairpins, with a single adenine, A5, involved in chain reversal. Dimerization involves head-to-head orientation of hairpins (Figures 2(a) and 7; Supplementary Material, Figure S1), with individual strands running antiparallel relative to their neighbors around the quadruplex (Figure 2(a)).

G·G·G·G tetrad

We detect a G3(*syn*)·G7(*anti*)·G3(*syn*)·G7(*anti*) alignment around the G·G·G·G tetrad in the dimeric d(GAGCAGGT) quadruplex. Such an alignment about the G·G·G·G tetrad is consistent with antiparallel alignment of adjacent strands around the quadruplex, and has been reported for the solution structures of the thrombin-binding DNA aptamer quadruplex,[27,28] as well as the d(GCGGT$_3$GCGG) Fragile X syndrome-containing sequence quadruplex[7] and the d(GGGCT$_4$GGGC) adeno-associated virus-containing sequence quadruplex.[10]

G·C·G·C tetrad

The G6·C4·G6·C4 tetrad (Figures 2(b) and 8(b)) is defined by all *anti* glycosidic torsion angles, consistent with antiparallel arrangement of adjacent strands around the dimeric d(GAGCAGGT) quadruplex. This type of direct G·C·G·C tetrad alignment (Figure 1(a)) has been observed previously for the solution structures of the d(GCGGT$_3$GCGG) Fragile X syndrome sequence-containing quadruplex[7] and the d(GGGCT$_4$GGGC) adeno-associated virus sequence-containing quadruplex.[10] There is, however, a critical distinction in that Watson-Crick G6·C4 pairs are formed between rather than within hairpin subunits (Figure 8(b)) in the head-to-head dimeric d(GAGCAGGT) quadruplex reported here. This contrasts with Watson-Crick G·C pairs within hairpin subunits in the head-to-tail dimeric d(GCGGT$_3$GCGG)[7] and d(GGGCT$_4$GGGC)[10] quadruplexes, reported previously.

The amino protons of C4 in the d(GAGCAGGT) quadruplex resonate at 8.49 ppm and 9.23 ppm. The chemical shift of 8.49 ppm is characteristic of a cytosine amino proton hydrogen-bonded to a carbonyl oxygen atom, such as would occur with a guanine residue in a Watson-Crick G·C pair. The chemical shift of 9.23 ppm is consistent with the other cytosine amino proton also being hydrogen bonded, and its much larger downfield shift may be reflective of its acceptors being both a ring nitrogen and carbonyl oxygen, such as would occur in a direct G·C·G·C tetrad (Figure 1(a)).

A·T·A·T tetrad

The slipped A2·T8·A2·T8 tetrad (Figures 2(d) and 8(c)) contains all *anti* glycosidic torsion angles, with hydrogen bonding along the major groove

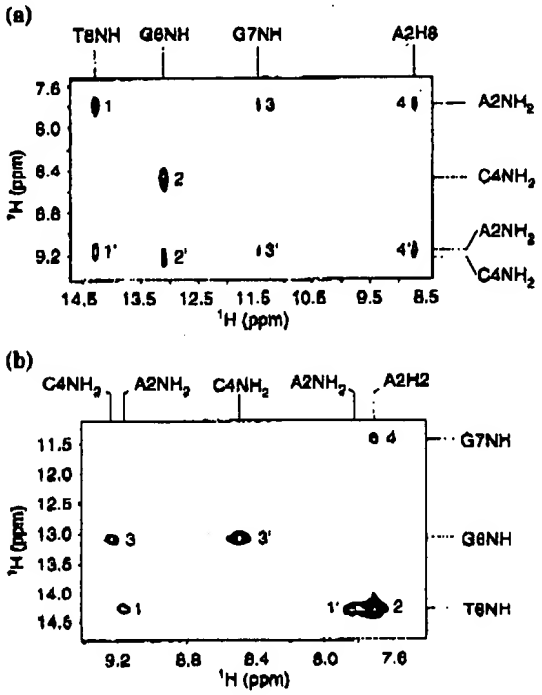

Figure 6. Identification of inter-strand NOEs. An expanded ^{15}N-edited (ω_1), ^{13}C, ^{15}N-purged (ω_2) NOESY (100 ms mixing time) contour plot of a 1:1 mixture of unlabeled and uniformly ^{13}C, ^{15}N-labeled d(GAGCAGGT) (5.3 mM in strands) in 1 M NaCl, 2 mM phosphate, H_2O (pH 6.6) at 0 °C. (a) Carrier is on amino-^{15}N. The relevant cross-peaks identifying inter-molecular NOEs are assigned as follows: 1,1', T8(NH3)-A2(NH_2-6); 2,2', G6(NH1)-C4(NH_2-4); 3,3', G7(NH1)-A2(NH_2-6); and 4,4', A2(H8)-A2(NH_2-6). (b) Carrier is on imino-^{15}N. The relevant cross-peaks identifying inter-molecular NOEs are assigned as follows: 1,1', T8(NH3)-A2(NH_2-6); 2, T8(NH3)-A2(H2); 3,3', G6(NH1)-C4(NH_2-4); 4, G7(NH1)-A2(H2).

edges of opposing adenine bases. This is the first report of any type (direct or slipped) of an A·T·A·T tetrad alignment, which involves pairing along the major groove edges. This A·T·A·T pairing alignment brings the H8 proton of one adenine in close proximity to the NH_2 proton of its adenine partner (Figure 1(d)), consistent with the observed intermolecular NOE between these pair of protons in mixed labeling experiments (peak 4 and 4', Figure 6(a)). Equally important, is our demonstration that Watson-Crick A2·T8 pairs are formed between rather than within hairpin subunits (Figure 8(c)) in the head-to-head dimeric d(GAGCAGGT) quadruplex.

The amino protons of A2 in the d(GAGCAGGT) quadruplex resonate at 7.80 ppm and 9.16 ppm. The chemical shift of 7.80 ppm is characteristic of an adenine amino proton hydrogen-bonded to a carbonyl oxygen atom, such as would occur with a thymine residue in a Watson-Crick A·T pair. The chemical shift of 9.16 ppm is consistent with the other adenine amino proton also being hydrogen bonded, and its much larger downfield shift is reflective of its acceptor being a ring nitrogen, such as would occur in a slipped A·T·A·T tetrad (Figure 1(d)).

Single base chain reversal

Chain reversal involves a single adenine, A5, within individual hairpin subunits (Figure 8(a)). The A5 base is bracketed by a closing G6·C4 mismatch involving pairing between the amino group of C4 and the acceptor atoms along the major groove edge of G6 (Figure 2(b)). This concept of a single base hairpin loop bracketed by a mismatch pair, was first reported for single base loops closed by sheared G·A mismatches in antiparallel duplexes.[29,30] There is no pairing between A5 residues across from each other (Figure 9(a)) in the head-to-head hairpin dimeric d(GAGCAGGT) quadruplex. Rather, the A5 residues are stacked over the adjacent C4 residues (Figure 9(a)).

We have checked for non-standard backbone torsion and sugar pucker pseudo-rotation (P) angles within the single residue edgewise turn spanning the C4-A5-G6 segment amongst the refined structures of the dimeric d(GAGCAGGT) quadruplex. For the C4-A5 step, the P value for C4

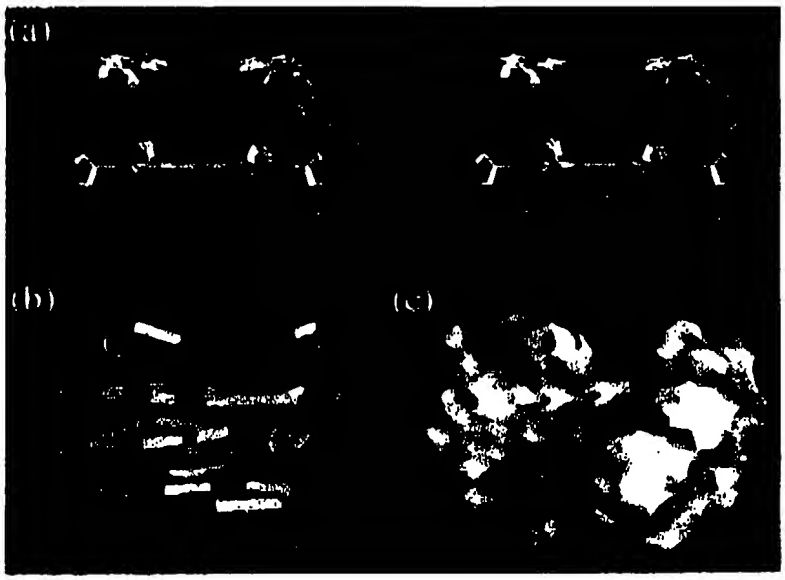

Figure 7. (a) Superpositioned stereo view of ten intensity refined structures of the dimeric d(GAGCAGGT) quadruplex. The backbones of the individual strands are in orange and green with phosphate oxygen atoms removed for clarity. The A5 residue is in white, the G6·C4·G6·C4 tetrad in magenta, G3·G7·G3·G7 tetrad in yellow and A2·T8·A2·T8 tetrad in cyan. (b) A GRASP ribbon view of a representative intensity refined structure of the d(GAGCAGGT) quadruplex. The backbones of individual strands are colored in blue and red. Guanine, adenine and thymine bases are colored yellow, red and blue, respectively. (c) A GRASP surface view of a representative intensity refined structure of the d(GAGCAGGT) quadruplex.

of 69.8(±5.7)° places it in the C4′-*exo* range, the γ value of 149.9(±40.1)° places it in the *trans* range (in contrast to standard *gauche*$^+$ value of 64°), and the χ value for A5 of 170.1(±4.6)° places it in the low *anti* range.

Base stacking

There is excellent pyrimidine/purine and purine/purine stacking between the bases of the direct G6·C4·G6·C4 tetrad (in magenta) and the G3·G7·G3·G7 tetrad (in yellow) in the folded topology of the d(GAGCAGGT) quadruplex (Figure 9(b)). We observe partial stacking between the bases of the G3·G7·G3·G7 tetrad (in yellow) and the slipped A2·T8·A2·T8 tetrad (in cyan) in the folded topology of the d(GAGCAGGT) quadruplex (Figure 9(c)). Overall, there is significant stacking of bases along the length of the dimeric d(GAGCAGGT) quadruplex.

The stacking pattern between the G3·G7·G3·G7 tetrad (in yellow) and the slipped A2·T8·A2·T8 tetrad (in cyan) (Figure 9(c)), positions the imino proton of G7 of one strand in close proximity to the NH_2 and H2 protons of A2 of the partner strand, consistent with the observed inter-strand NOEs (peaks 3 and 3′, Figure 6(a); peak 4, Figure 6(b)) in mixed labeling experiments.

Inter-strand NOEs

We have observed a set of weaker inter-strand NOEs, in addition to their stronger counterparts, shown in Figure 6(a) and (b), that merit further discussion. The studies presented in Figure 6 on an equimolar sample of unlabeled and uniformly ^{13}C,^{15}N-labeled d(GAGCAGGT) quadruplex in 1 M NaCl-containing H_2O buffer, were recorded at 0°C. We have also collected a ^{15}N-edited (ω_1), ^{13}C,^{15}N-purged (ω_2) NOESY[26] (100 ms mixing time) spectrum, with the carrier on the imino-^{15}N, recorded at 10°C. This spectrum had improved signal-to-noise, permitting data presentation at a lower contour level (as shown in Supplementary Material, Figure S7). We observe a set of weak inter-strand NOE cross-peaks labeled 5 to 9 in Supplementary Material, Figure S7, in addition to stronger peaks 1 to 4, that were also seen in Figure 6(b).

Peaks 5 and 5′, assigned to inter-strand NOEs between the imino proton of G7 and the amino protons of C4, are consistent with the stacking pattern shown in Figure 9(b). Peaks 6 and 6′, assigned to inter-strand NOEs between the imino proton of G7 and the amino protons of A2, are consistent with the stacking pattern shown in Figure 9(c). Peak 9, assigned to an inter-strand NOE between the imino of G6 and the H2 of A5, is consistent with the stacking pattern shown in Figure 9(a).

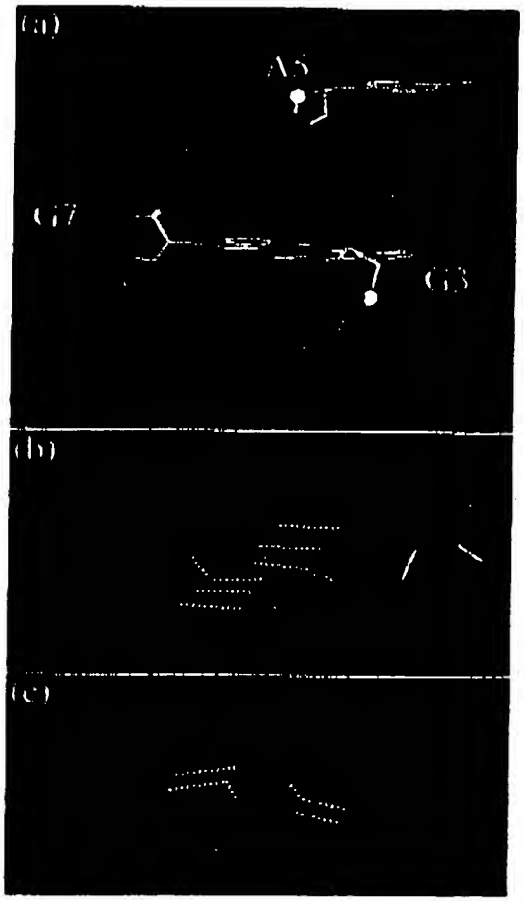

Figure 8. (a) A stick representation of a symmetric half (corresponding to one of the two strands) of a representative intensity refined structure of the d(GAGCAGGT) quadruplex. The color code is the same as outlined in the legend to Figure 7. (b) Pairing alignment of the G6·C4·G6·C4 tetrad. (c) Pairing alignment of the A2·T8·A2·T8 tetrad.

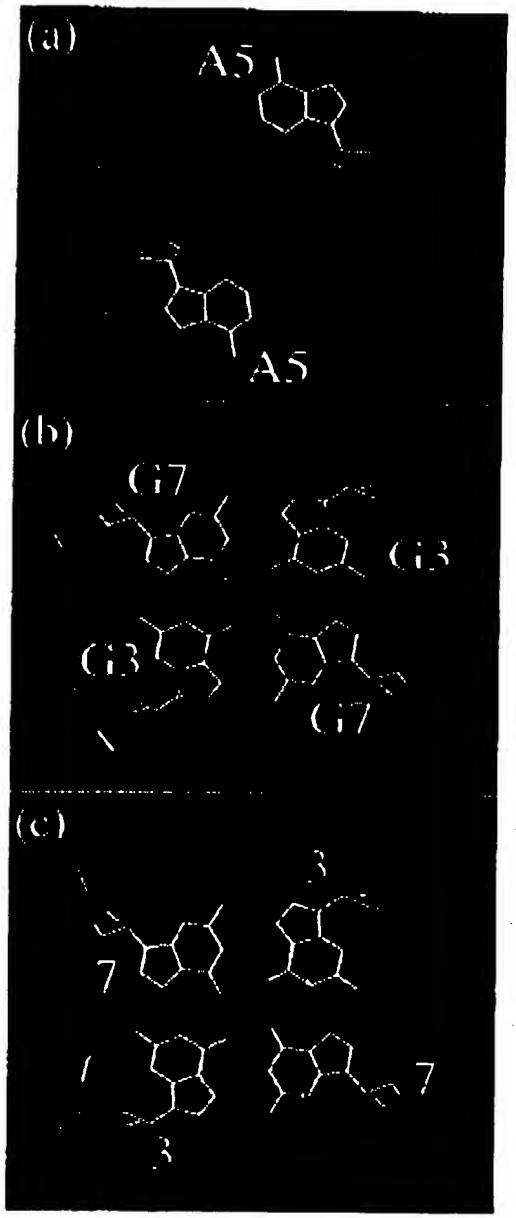

Figure 9. Base stacking overlap patterns in a representative intensity refined structure of the d(GAGCAGGT) quadruplex. (a) Stacking of A5 (in white) on the G6·C4·G6·C4 tetrad (in magenta). (b) Stacking of the G6·C4·G6·C4 tetrad (in magenta) on the G3·G7·G3·G7 tetrad (in yellow). (c) Stacking of the G3·G7·G3·G7 tetrad (in yellow) on the A2·T8·A2·T8 tetrad (in cyan).

By contrast, peak 7 assigned to an inter-strand NOE between the imino of G3 and the H8 of A2, cannot be explained by the overlap pattern in Figure 9(c); Peak 8, representing an inter-strand NOE assigned to the imino of G3 and the H8 proton of G6/G7, cannot be explained by the overlap pattern shown in Figure 9(b). In both cases, while the inter-strand distances between proton pairs are long, their intra-strand counterparts are in close proximity. Thus, it could be argued that perhaps peaks 7 and 8 reflect relatively strong intra-strand NOEs that are not completely removed by isotope filtering. For this xplanation to be valid, peaks 7 and 8 should have been doublets, because ^{13}C decoupling was not acquired during acquisition. Currently, we are somewhat at a loss to account for this discrepancy involving weak peaks 7 and 8 (Supplementary Material, Figure S7), whose inten-

sity did vary in the weak range when the experiments were checked for reproducibility.

Salt dependence

The broad resonances for the d(GAGCAGGT) sequence in low NaCl solution (Supplementary Material, Figure S3(a)) is indicative of aggregate formation. What was unexpected was the transition to narrow resonances in 1 M NaCl solution (Supplementary Material, Figure S3(b)), resulting in the formation of a dimeric d(GAGCAGGT) quadruplex, amenable to structural characterization. Both the direct G·C·G·C (Figure 1(a)) and slipped A·T·A·T (Figure 1(d)) tetrads have inwardly pointing amino groups, an alignment not conducive to coordinating monovalent cations positioned either between or within tetrad planes. Therefore, it is conceivable that 1 M NaCl has minimal effect on the integrity of the dimeric d(GAGCAGGT) quadruplex, but for some unknown reason may destabilize the aggregated species that predominates in low salt solution.

Comparison with mixed tetrads involving minor groove alignment of G·C and A·T pairs

Our structural studies on major groove-aligned direct G·C·G·C and slipped A·T·A·T tetrads in the head-to-head dimeric d(GAGCAGGT) quadruplex (this study) can be compared with reported structural studies on quadruplexes involving minor groove-aligned direct G·C·G·C (Supplementary Material, Figure S1(a)) and slipped cation-coordianted A·T·A·T (Supplementary Material, Figure S1(b)) tetrads formed by dimerization of linear and cyclic octameric sequences.[8,9,14] Interestingly, the minor groove-aligned direct G·C·G·C (Supplementary Material, Figure S1(a)) and slipped cation-coordinated A·T·A·T (Supplementary Material, Figure S1(b)) tetrads also involve Watson-Crick G·C and A·T pairing between rather than within head-to-head hairpin dimers of the quadruplex.

It should be noted that while the major groove-aligned direct G·C·G·C (Figure 1(a)) and slipped A·T·A·T (Figure 1(d)) tetrads adopt planar geometries in the solution structure of the dimeric d(GAGCAGGT) quadruplex (this study), the minor groove-aligned direct G·C·G·C (Supplementary Material, Figure S2(a)) and slipped cation-coordianted A·T·A·T (Supplementary Material, Figure S2(b)) tetrads adopt distinctly non-planar geometries within their quadruplexes, both in the crystalline[8,14] and solution[9] states.

Biological relevance

We have reported the first experimental demonstration for formation of a major groove-aligned slipped A·T·A·T tetrad (Figure 1(d)) within a DNA quadruplex architecture. This result, together with our previous demonstration of major groove-aligned direct G·C·G·C tetrad (Figure 1(a))[7] formation within a quadruplex architecture, expands on the code for alignment of duplex segments that can potentially participate in strand exchange during homologous recombination. The glycosidic bonds are directed outwards in major groove aligned tetrads (Figure 1), while they are directed inwards in minor groove-aligned tetrads (Supplementary Material, Figure S1). There is steric crowding between the inwardly pointing sugars in the minor groove-aligned tetrads, resulting in base-sugar and sugar-sugar interactions which severely buckle the planes of the tetrads.[8,9,13] By contrast, there is no such crowding between the outwardly pointing sugars in the major groove-aligned mixed tetrads, resulting in a planar arrangement of bases within the tetrad. Several challenges remain despite our identification here of a major groove-aligned slipped A·T·A·T tetrad (Figure 1(d)) at one end of a quadruplex. Can one identify formation of a major groove-aligned direct A·T·A·T tetrad (Figure 1(c)), and can either the direct or slipped A·T·A·T tetrads be positioned in the interior of the quadruplex?

McGavin[31] was the first to recognize the potential for self-pairing of Watson-Crick G·C and A·T pairs to form dyad axes related major groove-aligned G·C·G·C and A·T·A·T tetrads. Such tetrad-based quadruplexes could play a role in strand exchange between two homologous duplexes during genetic recombination. Wilson[32] next proposed a quadruplex-based model for formation of reciprocal heteroduplexes from their homologous duplex counterparts. In this model, homologous duplexes initially associate through G·C·G·C and A·T·A·T tetrad formation along their minor groove edges, placing complementary strands opposite each other. Strand exchange can then occur following a 90° rotation of each base, such that the base-pairs now face each other through G·C·G·C and A·T·A·T tetrad formation along their major groove edges. Experimental studies[33,34] have provided evidence for quadruplex formation by poly(CA)$_n$·poly(TG)$_n$ repeats, while computational studies[35] have established that such strand exchange quadruplexes, as well as quadruplex-duplex junctions, are stereochemically robust and form stable entities. Thus, a future challenge would be to design a DNA quadruplex consisting solely of G·C·G·C and A·T·A·T tetrads and attempt to trap structures where the alignment is through the minor groove on the one hand, and through the major groove on the other.

Materials and Methods

Preparation of unlabeled and uniformly ^{13}C, ^{15}N-labeled DNA

The unlabeled d(GAGCAGGT) sequence was synthesized on a 10 μmol scale on an Applied Biosystems 392 DNA synthesizer using solid phase β-cyanoethyl-

phosphoamidite chemistry and was subsequently purified by high pressure liquid chromatography (HPLC).

A modified version of the Zimmer & Crothers[26] procedure as described[19,26] was used for the enzymatic synthesis of uniformly $^{13}C,^{15}N$-labeled d(GAGCAGGT) sequence. The in-house prepared uniformly $^{13}C,^{15}N$-labeled dNTPs[19,26] were used as building blocks in the *in vitro* polymerization reaction catalyzed by murine mammary leukemia virus (MMLV) reverse transcriptase (Gibco-BRL). The uniformly $^{13}C,^{15}N$-labeled d(GAGCAGGT) 8-mer was separated from the unlabeled 24-mer template using 22% (w/v) denaturing polyacrylamide electrophoresis. The DNA 8-mer bands were eluted from the gel by "crush and soak" procedure and purified as described above for the non-labeled samples.

NMR data collection and processing

NMR data on the d(GAGCAGGT) 8-mer in H_2O and ^2H_2O buffer (1 M NaCl, 2 mM phosphate (pH 6.6)) were collected on a Varian 600 MHz Unity *Inova* NMR spectrometer. Proton assignments are based on homonuclear NOESY, correlation spectroscopy (COSY), TOCSY and HCCNH-TOCSY experiments. Data sets were processed and analyzed using the FELIX program (Molecular Simulations).

Two bond $^{2h}J_{NN}$ scalar couplings between imino and amino donors and nitrogen acceptors in uniformly $^{13}C,^{15}N$-labeled d(GAGCAGGT) in 1 M NaCl were monitored in HNN-COSY[21,22] and H(CN)N(H)[24,25] contour plots using pulse sequences described in the literature.

Distance restraints

The distances between non-exchangeable protons were estimated from the buildup curves of cross-peak intensities in NOESY spectra at four different mixing times (50, 150, 200 and 250 ms) in ^2H_2O and given bounds of ±30% with distances referenced relative to the cytosine H6-H5 distance of 2.47 Å. Exchangeable proton restraints are based on NOESY data sets at two mixing times (60 and 200 ms) in H_2O. Cross-peaks involving exchangeable protons were classified as strong (medium to strong intensity at 60 ms), medium (weak intensity at 60 ms) and weak (observed only at a mixing time of 200 ms) and proton pairs were then restrained, respectively, to distances of 3.0(±0.9) Å, 4.0(±1.2) Å and 6.0(±1.8) Å. Since the experimental NMR data are consistent with a dimeric quadruplex motif, non-crystallographic symmetry restraints were imposed on all heavy atoms.

Structure calculations

The structure of the d(GAGCAGGT) in 1 M NaCl was determined by molecular dynamics (MD)-simulated annealing computations driven by NOE distance and hydrogen bonding restraints using the X-PLOR package, version 3.8.[27] At the initial stage of the refinement, torsional molecular dynamics was undertaken at high temperature. The molecules were equilibrated at 20,000 K (30,000 steps over 3 ps) and then cooled very slowly to 1000 K (40,000 steps over 20 ps). The potential energy function included a repulsive force field, NOE and hydrogen bond distance restraints, glycosidic bond (χ) dihedral angle restraints and a non-crystallographic symmetry potential. The force constant for NOE distance restraints was maintained at a value of 30 kcal mol^{-1} Å^{-2}, while for hydrogen bonds restraints the value was 50 kcal mol^{-1} Å^{-2}. All NOE distance restraints were considered as ambiguous and treated with the "sum" averaging option.[34,39] Dihedral angle restraints (210(±40)°, with force constant of 50 kcal mol^{-1} rad^{-2}) were imposed on glycosidic torsion angles for the residues A2, C4, A5, G6, G7 and T8 shown experimentally to adopt *anti* conformations. Dihedral angle restraints (65(±40)°, with force constant of 50 kcal mol^{-1} rad^{-2}) were imposed on glycosidic torsion angles for the G3 residue shown experimentally to adopt *syn* conformation. The force constant for non-crystallographic symmetry was maintained at 30 kcal mol^{-1} Å^{-2}.

These computations were followed by lower temperature Cartesian space molecular dynamics guided by the hydrogen bonding and NOE distance restraints with changes in the potential energy function: the repulsive force field was replaced with Lennard-Jones potentials and planarity restraints were included for tetrad planes with low weights of 5 kcal mol^{-1} Å^{-2} and 10 kcal mol^{-1} Å^{-2}, respectively. During this stage of the dynamics, the structures were further cooled from 1000 K to 300 K (20,000 steps over 10 ps) and minimized until the gradient of energy was less than 0.1 kcal mol^{-1}. It should be noted that computations repeated without planarity restraints resulted in the same low energy structures, but exhibited a lower convergence rate.

The refinement protocol started from 60 different initial structures. The initial structures were generated as sets of two chains, each eight nucleotides long, randomized for all dihedral angles, and separated by space intervals of 50 Å. The convergence rate following dynamics was good for the case where the computations were guided by hydrogen bonding restraints associated with the topology shown in Figure 2(a): Sixteen structures out of 60 emerged with the same fold and pairwise r.m.s.d. values less than 1.0 Å between members of the group. Non-converged structures were separated from that group by large gaps (in total more than 400 kcal) in all components of the potential energy (van der Waals, NOE violations, covalent geometry).

The ten converged distance refined structures corresponding to the folding topology shown schematically in Figure 1(a) were used as the starting point for subsequent X-PLOR based energy minimization with back-calculation of the NOESY spectra. The relaxation matrix was set up for the non-exchangeable protons, with the exchangeable imino and amino protons exchanged for deuterons. A total of 712 non-exchangeable intensity values from NOESY data sets at four mixing times in ^2H_2O buffer (178 non-exchangeable intensities per mixing time) were included with force constant of 500 kcal mol^{-1}. The planarity restraints were set to very low values of 1.0 kcal Å^{-2} for the G·G·G·G tetrad and 0.5 kcal Å^{-2} for the A·T·A·T and G·C·G·C tetrads. The distance restraints were retained with 30% bounds and the same weights as before. During minimization, the NMR R factor ($R_{1/6}$) improved from the initial value of 12% to 7.4% while retaining structure convergence and stereochemistry.

Coordinates deposition

Coordinates (accession number: 1jvc) of the dimeric d(GAGCAGGT) quadruplex have been deposited in the RCSB Protein Data Bank.

Acknowledgments

This research was supported by NIH grants GM-34504 to D.J.P.

References

1. Williamson, J. R. (1994). G-quartet structures in telomeric DNA. *Annu. Rev. Biophys. Biomol. Struct.* **23**, 703-730.
2. Rhodes, D. & Giraldo, R. (1995). Telomere structure and function. *Curr. Opin. Struct. Biol.* **5**, 311-312.
3. Feigon, J., Koshlap, K. M. & Smith, F. W. (1995). ^{1}H NMR spectroscopy of DNA triplexes and quadruplexes. *Methods Enzymol.* **261**, 225-255.
4. Patel, D. J., Bouaziz, S., Kettani, A. & Wang, Y. (1999). Structures of guanine-rich and cytosine-rich quadruplexes formed *in vitro* by telomeric, centromeric and triplet repeat disease sequences. *Oxford Handbook of Nucleic Acid Structures* (Neidle, S., ed.), pp. 389-453, Oxford University Press, Oxford.
5. Arthanari, H & Bolton, P. H. (2001). Functional and dysfunctional roles of quadruplex DNA in cells. *Chem. Biol.* **8**, 221-230.
6. Sen, D. & Gilbert, W. (1991). The structure of telomeric DNA: DNA quadruplex formation. *Curr. Opin. Struct. Biol.* **1**, 435-438.
7. Kettani, A., Kumar, R. A. & Patel, D. J. (1995). Solution structure of a DNA quadruplex containing the fragile X syndrome triplet repeat. *J. Mol. Biol.* **254**, 636-656.
8. Leonard, G. A., Zhang, S., Peterson, M. R., Harrop, S. J., Helliwell, J. R., Cruse, W. B. *et al.* (1995). Self-association of a DNA loop creates a quadruplex crystal structure of d(GCATGCT) at 1.8 Å resolution. *Structure*, **3**, 335-340.
9. Escaja, N., Fedroso, E., Rico, M. & Gonzalez, C. (2000). Dimeric solution structure of two cyclic octamers. Four-stranded DNA structures stabilized by A·T·A·T and G·C·G·C tetrads. *J. Am. Chem. Soc.* **122**, 12732-12742.
10. Kettani, A., Bouaziz, S., Gorin, A., Zhao, H., Jones, R. & Patel, D. J. (1998). Solution structure of a Na^+ cation stabilized DNA quadruplex containing G·G·G·G and G·C·G·C tetrads formed by G-G-G-C repeats observed in adeno-associated viral DNA. *J. Mol. Biol.* **282**, 619-636.
11. Bouaziz, S., Kettani, A., Zhao, H., Jones, R. & Patel, D. J. (1998). A K^+ cation dependent conformational switch within a loop spanning segment of a DNA quadruplex containing G-G-G-C repeats. *J. Mol. Biol.* **282**, 637-652.
12. Majumdar, A , Kettani, A., Skripkin, E. & Patel, D. J. (2001). Pulse sequences for detection of $NH_2\cdots N$ hydrogen bonds in a sheared G·A mismatches *via* remote, nonexchangeable protons. *J. Biomol. NMR*, **19**, 103-113.
13. Salisbury, S. A., Wilson, S. E., Powell, H. R., Kennard, O., Lubini, P., Sheldrick, G. M. *et al.* (1997). The bi-loop, a new general four-stranded DNA motif. *Proc. Natl Acad. Sci. USA*, **94**, 5515-5518.
14. Kuryavyi, V. V. & Jovin, T. M. (1995). Triad-DNA: a model for trinucleotide repeats. *Nature Genet.* **9**, 339-341.
15. Kettani, A., Bouaziz, S., Wang, W., Jones, R. A. & Patel, D. J. (1997). *Bombyx mori* single repeat telomeric DNA sequences forms a G-quadruplex capped by base triads. *Nature Struct. Biol.* **4**, 382-389.
16. Kettani, A., Basu, G., Gorin, A., Majumdar, A., Skripkin, E. & Patel, D. J. (2000). A two-stranded template-based approach to G·(C-A) triad formation: designing novel structural elements into an existing DNA framework. *J. Mol. Biol.* **301**, 129-146.
17. Kuryavyi, V., Kettani, A., Wang, W., Jones, R. & Patel, D. J. (2000). A diamond-shaped zipper-like DNA architecture containing triads sandwiched between mismatches and tetrads. *J. Mol. Biol.* **295**, 455-469.
18. Kuryavyi, V., Majumdar, A., Shallop, A., Chernichenko, N., Skripkin, E., Jones, R. A. & Patel, D. J. (2001). A double chain reversal loop and two diagonal loops define the architecture of a unimolecular DNA quadruplex containing a pair of stacked G(*syn*)· G(*syn*)· G(*anti*)· G(*anti*) tetrads flanked by a G·(T-T) triad and a T·T·T triple. *J. Mol. Biol.* **310**, 181-194.
19. Kettani, A., Gorin, A., Majumdar, A., Hermann, T., Skripkin, E., Zhao, H. *et al.* (2000). A dimeric DNA interface stabilized by A·(G·G·G·G)·A hexads and coordinated monovalent cations. *J. Mol. Biol.* **297**, 627-644.
20. Phan, A. T. (2000). Long range imino proton-^{13}C-J couplings and the through-bond correlation of imino and non-exchangeable protons in unlabeled DNA. *J. Biomol. NMR*, **16**, 175-178.
21. Dingley, A. J. & Grzesiek, S. (1998). Direct observation of hydrogen bonds in nucleic acid base-pairs by internucleotide $^2J_{NN}$ couplings. *J. Am. Chem. Soc.* **120**, 8293-8297.
22. Pervushin, K., Ono, A., Fernandez, C., Szyperski, T., Kainosho, M. & Wuthrich, K. (1998). NMR scalar couplings across Watson-Crick base-pair hydrogen bonds in DNA observed by transverse relaxation-optimized spectroscopy. *Proc. Natl Acad. Sci. USA*, **95**, 14147-14151.
23. Majumdar, A., Kettani, A. & Skripkin, E. (1999). Observation and measurement of $^2J_{NN}$ coupling constants between ^{15}N nuclei with widely separaterd chemical shifts. *J. Biomol. NMR*, **14**, 67-70.
24. Majumdar, A., Kettani, A. & Skripkin, E. (1999). Observation of internucleotide N-H··N hydrogen bonds in the absence of directly detectable protons. *J. Biomol. NMR*, **15**, 207-211.
25. Hennig, M. & Williamson, J. R. (2000). Detection of N-H··N hydrogen bonding in RNA via scalar couplings in the absence of observable imino proton resonances. *Nucl. Acids Res.* **28**, 1585-1593.
26. Kettani, A., Bouaziz, S., Skripkin, E., Majumdar, A., Wang, W., Jones, R. A. & Patel, D. J. (1999). Interlocked mismatch-aligned arrowhead DNA motifs. *Structure*, **7**, 803-815.
27. Macaya, R. F., Schultze, P., Smith, F. W., Roe, J. A. & Feigon, J. (1993). Thrombin-binding DNA aptamer forms a unimolecular quadruplex structure in solution. *Proc. Natl Acad. Sci. USA*, **90**, 3745-3749.
28. Wang, K. Y., Krawczyk, S. H., Bischofberger, N., Swaminathan, S. & Bolton, P. H. (1993). The tertiary structure of a DNA aptamer which binds to and inhibits thrombin determines activity. *Biochemistry*, **32**, 11285-11292.
29. Chou, S. H., Zhu, L., Gao, Z., Cheng, J-W. & Reid, B. R. (1996). Hairpins loops consisting of single adenine residues closed by a sheared A·A and G·G pairs formed by the DNA triplets AAA and GAG:

Solution structure of the d(GTACAAAGTAC). *J. Mol. Biol.* 264, 981-1001.

30. Hirao, I., Kawai, G., Yoshizawa, S., Nishimura, Y., Ishido, Y., Watanabe, K. & Miura, K. (1994). Most compact hairpin turn structure exerted by a short DNA fragment d(GCGAAGC) in solution: an extraordinarily stable structure resistant to nucleases and heat. *Nucl. Acids Res.* 22, 576-582.
31. McGavin, S. (1971). Models of specifically paired like (homologous) nucleic acid structures. *J. Mol. Biol.* 55, 293-298.
32. Wilson, J. H. (1979). Nicked-free formation of reciprocal heteroduplexes: a simple solution to the topological problem. *Proc. Natl Acad. Sci. USA*, 76, 3641-3645.
33. Johnson, D. & Morgan, A. R. (1978). Unique structures formed by pyrimidine·purine DNA which may be four-stranded. *Proc. Natl Acad. Sci. USA*, 75, 1637-1641.
34. Gaillard, C. & Strauss, F. (1994). Association of poly(CA)·poly(TG) DNA fragments into four-stranded complexes bound by HMG1 and 2. *Science*, 264, 433-436.
35. Lebrun, A. & Lavery, R. (1995). Modeling a strand exchange tetraplex conformation. *J. Biomol. Struct. Dynam.* 13, 459-464.
36. Zimmer, D. P. & Crothers, D. M. (1995). NMR of enzymatically synthesized uniformly ^{13}C, ^{15}N-labeled DNA oligonucleotides. *Proc. Natl Acad. Sci. USA*, 92, 3091-3095.
37. Brunger, A. T. (1992). *X-PLOR. A System for X-ray Crystallography and NMR*, Yale University Press, New Haven, CT.
38. Nilges, M. (1995). Calculation of protein structures with ambiguous distance restraints. Automated assignment of ambiguous NOE cross-peaks and disulfide connectivities. *J. Mol. Biol.* 245, 645-660.
39. Nilges, M., Habazettl, J., Brunger, A. T. & Holak, T. A. (1991). Relaxation matrix alignment of the solution structure of squash trypsin inhibitor. *J. Mol. Biol.* 219, 499-510.

Edited by M. F. Summers

(Received 22 May 2001; received in revised form 8 August 2001; accepted 8 August 2001)

http://www.academicpress.com/jmb

Supplementary Material for this paper comprising seven Figures and two Tables are available on IDEAL